

On the efficacy of higher-order spectral clustering under weighted stochastic block models

Xiao Guo[†], Hai Zhang[†], Xiangyu Chang^{‡*}

[†] School of Mathematics, Northwest University, China

[‡] School of Management, Xi'an Jiaotong University, China

June 6, 2025

Abstract

Higher-order structures of networks, namely, small subgraphs of networks (also called network motifs), are widely known to be crucial and essential to the organization of networks. Several works have studied the community detection problem—a fundamental problem in network analysis at the level of motifs. In particular, the higher-order spectral clustering has been developed, where the notion of *motif adjacency matrix* is introduced as the algorithm's input. However, how the higher-order spectral clustering works and when it performs better than its edge-based counterpart remain largely unknown. To elucidate these problems, the higher-order spectral clustering is investigated from a statistical perspective. The clustering performance of the higher-order spectral clustering is theoretically studied under a *weighted stochastic block model*, and the resulting bounds are compared with the corresponding results of the edge-based spectral clustering. The upper bounds and simulations show that when the network is dense with the weak signal of weights, higher-order spectral clustering can lead to a performance gain in clustering. Real data experiments also corroborate the merits of higher-order spectral clustering.

Keywords: Higher-order structures, Community detection, Weighted networks, Network motifs

*Xiangyu Chang is the corresponding author.

1 Introduction

The network is a standard representation of relationships among units of complex systems in many scientific domains, including biology, ecology, sociology, and information science, among many others (Newman, 2018; Goldenberg et al., 2010; Kolaczyk, 2009). One of the most common features of networks is that they have communities, clusters, or modules—groups of nodes that are, in some sense, more similar to nodes within the same community than to other nodes. Community detection, namely, detecting such communities based on given network structures, has been one of the fundamental problems in network analysis which helps us gain knowledge about the behavior and functionality of networks.

Past decades have seen various community detection methods, including spectral clustering, modularity maximization, likelihood methods, and semidefinite programming. See Abbe (2018) for a survey. Most of the current community detection procedures are edge-based, that is, those procedures essentially make use of the network adjacency matrix, which stores the similarity of each pair of nodes to detect communities. However, there has been increasing evidence that *higher-order* connectivity patterns are crucial to the organization of real networks. They can help understand and gain more insights into the behavior of networks (Holland and Leinhardt, 1977; Milo et al., 2002; Mangan et al., 2003; Yang and Leskovec, 2014; Rosvall et al., 2014). The higher-order structures of networks often refer to small network subgraphs, or the so-called network *motifs*, in contrast to the *lower-order* network edges. In particular, triangular motifs are common in many kinds of networks. For example, in social networks, individuals who share a common friend are more likely to become friends, leading to a large proportion of triangles to the two-edge wedges (Rohe and Qin, 2013).

Very recently, several works have studied the problem of network clustering at the level of motifs, which can provide new insights into network organization beyond the edge-based clustering if the network exhibits rich higher-order structures; see Benson et al. (2016); Tsourakakis et al. (2017); Laenen and Sun (2020); Underwood et al. (2020), among others. Generally, to capture the higher-order connective patterns, a *motif adjacency matrix* is often

designed as a surrogate for the original edge adjacency matrix; see [Benson et al. \(2016\)](#); [Paul et al. \(2018\)](#) for example. To be specific, the (i, j) 's entry of the motif adjacency matrix is the number of certain motifs that nodes i and j participate in commonly in binary networks. It is suggested that one could use the motif adjacency matrix in the subsequent clustering analysis to obtain a good empirical result. In particular, the *higher-order spectral clustering*, namely, the spectral clustering with the motif adjacency matrix as its input, is well-suited to the problem and is the focus of this work. However, it remains largely unknown how higher-order spectral clustering actually works. Moreover, when it is better than its edge-based counterpart remains to be seen. From a statistical perspective, the aim should be to show the efficacy of higher-order spectral clustering on a particular network dataset and to understand its merits under some underlying mechanisms.

In this paper, we attempt to illustrate the efficacy of higher-order spectral clustering in the context of weighted networks. To this end, we develop the *weighted stochastic block models* (WSBMs) to mimic the weighted networks with communities, which is a generalization of the stochastic block models (SBMs) ([Holland et al., 1983](#)) to weighted networks. In particular, we assume the edges are first generated according to the SBM mechanism, where nodes are partitioned into several distinct communities and conditioned on the underlying community assignments. The edges are generated independently according to the community membership of their end nodes. After that, positive weights independently generated from a common distribution are assigned to all the existing edges. We specify the expectation of weights without requiring their distributions. As a generalization of the aforementioned motif adjacency matrix, we define the *weighted motif adjacency matrix* to capture the network weights, whose (i, j) 's entry is the weights summation of a certain motif that nodes i and j both involve. In particular, we focus on the undirected triangular motif. With these at hand, we study the approximation error and misclustering error of the higher-order spectral clustering under the WSBM mechanism and compare the upper bounds with the corresponding results of edge-based spectral clustering (i.e., spectral clustering with the weighted edge adjacency matrix as the input). It turns out that when the network is dense *but* the conditional expectation of edge weight is small, and the higher-

order spectral clustering leads to a lower misclustering error than the edge-based one does. The rationality is as follows. The signal of communities could be weak under small edge weight, which may lead to unsatisfactory clustering performance of the edge-based method. However, when the network is dense, the triangles are rich, which enables each node pair to borrow the strength and information of incident edges. Thus, the clustering quality could be improved by utilizing the triangular motif. Note that the unequal weights are crucial to ensure the advantage of the higher-order spectral clustering over the edge-based one. In addition, it is worth noting that, theoretically, the weighted motif adjacency matrix leads to a larger eigen-gap of the corresponding population matrix than the edge adjacency matrix does. In this sense, the signals of the weighted networks are thus enhanced. We conduct simulations to verify the theoretical findings. In particular, the higher-order spectral clustering has performance gain over the edge-based counterpart in various regimes where the requirements for theory are not necessarily met. The real data experiments on two statisticians networks and one PM_{2.5} network provide insightful and interesting results, showing the efficacy of higher-order spectral clustering on weighted networks.

The remainder of this paper is organized as follows. Subsection 1.1 reviews the related works. Section 2 provides the general framework including the notation, weighted stochastic block models and higher-order spectral clustering. Section 3 presents the theoretical results. Section 4 discusses the theoretical and methodological aspects of our work and also poses possible extensions. Sections 5 and 6 include the simulations and real data analysis, respectively. Section 7 concludes the paper. The proofs can be found in the Supplementary Material.

1.1 Related works

Analyzing networks at the level of motifs has received increasing attention in recent years. In particular, [Benson et al. \(2016\)](#) proposed a conductance-based method, which generalized the original edge-based conductance to the motif-based one. The motif adjacency matrix was then introduced to simplify the minimization of the motif-based conductance; more specifically, minimizing the motif-based conductance can be reduced to minimizing the

edge-based conductance but using the motif adjacency matrix. [Serroux et al. \(2011\)](#) studied the higher-order network clustering in the modularity maximization framework, where they generalized the notion of modularity by transforming its building block from edges to motifs. They employed the tensor to capture the triangular patterns within the network but then transformed it to the aforementioned motif adjacency matrix to accelerate the algorithm. There are also works focusing on directed networks ([Laenen and Sun, 2020](#); [Cucuringu et al., 2020](#); [Underwood et al., 2020](#)) and local spectral clustering ([Yin et al., 2017](#)).

The statistical aspects of the motif-based methods are also studied by several authors. [Rohe and Qin \(2013\)](#) show the blessings of transitivity in sparse networks. They developed an algorithm that exploits the triangles built by network transitivity and shows its clustering ability statistically under the newly developed local stochastic block models. [Tsourakakis et al. \(2017\)](#) also studied the motif-based conductance and provided a random walk explanation of it. They showed that the random walk on the network corresponding to the motif adjacency matrix is more likely to stay in the same true community of the stochastic block model ([Holland et al., 1983](#)) than the random walk on the original network. [Paul et al. \(2018\)](#) proposed a superimposed stochastic block model, which is a superimposition of a classical dyadic (edge-based) random graph and a triadic (triangle-based) random graph. They rigorously analyzed the misclustering error bound of the higher-order spectral clustering under such models. However, the analysis fails to disclose the advantage of higher-order spectral clustering over the edge-based counterpart. In addition, the model is somewhat restrictive since the networks generated by the superimposed stochastic block models have edges lying in $\{0, 1, 2\}$, which infrequently happens in real networks. [Cucuringu et al. \(2020\)](#) studies the spectral clustering on complex-valued Hermitian matrix representations, which implicitly use the higher-order structure of directed networks. They studied the algorithm theoretically under stochastic block models.

There exists another line of works focusing on the hyper-graph clustering problem; see [Ghoshdastidar et al. \(2017\)](#); [Ghoshdastidar and Dukkipati \(2017, 2014\)](#), among many others. In hyper-graphs, the hyper-edges are directly known as a prior rather than constructed using the motifs. Theoretically, the motif adjacency matrix brings extra dependence be-

tween entries. Nevertheless, in the context of hyper-graph clustering, the entries of the adjacency tensor are independent.

There are also some authors making use of the motifs to study the testing problem of whether it has only one community or multiple communities under SBMs or its variants; notably by [Jin et al. \(2018\)](#); [Gao et al. \(2017\)](#); [Jin et al. \(2021\)](#); [Cammarata and Ke \(2022\)](#).

On the other hand, there exist a few works on community detection for weighted networks; see [Aicher et al. \(2015\)](#); [Xu et al. \(2020\)](#); [Cerqueira and Levina \(2023\)](#) for example and references therein. Compared with these works, we are motivated to enhance the signal strength in weighted networks by using the weighted motif adjacency matrix and studying its effect theoretically. Generally, using the weighted motif adjacency matrix can be regarded as a network preprocessing step, and the weighted motif adjacency matrix can essentially be the input of other community detection algorithms.

2 Framework

In this section, we introduce the general framework of analysis. In particular, the WSBMs and the higher-order spectral clustering are introduced.

We first introduce some notes and notation. The readers could also refer to [Table 1](#) for a brief summary. $\mathbb{M}_{n,K}$ denotes the set of all $n \times K$ matrices which have exactly one 1 and $K - 1$ 0's in each row. Any $\Theta \in \mathbb{M}_{n,K}$ is called a *membership matrix*, where each row corresponds to the community membership of the corresponding node. For example, node i belongs to community $g_i \in \{1, \dots, K\}$ if and only if $\Theta_{ig_i} = 1$. For $1 \leq k \leq K$, denote $G_k = G_k(\Theta) = \{1 \leq i \leq n : g_i = k\}$ and $n_k = |G_k|$, where G_k consists of nodes with their community membership being k . For any matrix $A_{n \times n}$ and $I, J \subseteq \{1, \dots, n\}$, A_{I*} and A_{*J} denote the submatrix of A consisting of the corresponding rows and columns of A , respectively. $\|A\|_F$, $\|A\|_2$, and $\|A\|_\infty$ denote the Frobenius norm, spectral norm, and the element-wise maximum absolute value of A , respectively. $\text{diag}(A)$ denotes the diagonal matrix with its diagonal elements being the same as those of A . We also use $\|a\|_2$ to denote the Euclidean norm of any vector a .

Now we introduce the WSBMs which generalizes the SBMs ([Holland et al., 1983](#)) such

that the potential network can have weighted edges rather than the binary edges in the SBMs. For an underlying network with n nodes and K communities, the two main parameter matrices of the WSBMs are the membership matrix $\Theta \in \mathbb{M}_{n,K}$, and the connectivity matrix $B \in [0, 1]^{K \times K}$ where B is of full rank, symmetric, and the entry B_{kl} of B represents the edge probability between any node in community l and any node in community k . For simplicity, throughout the paper we assume the underlying network has balanced community size n/K with the within-community probability being p_n and the between-community probability being $p_n(1 - \lambda)$ for any pair of nodes, where λ is a constant in $(0, 1)$. Whereas note that the theoretical results, say the approximation error bound to be established in Theorem 1, also holds for general B 's; see Remark 3. Under the simplified structural assumption, the connectivity matrix B takes the simple form

$$B = p_n \lambda I_K + p_n(1 - \lambda) \mathbf{1}_K \mathbf{1}_K^\top, \quad (2.1)$$

where $\mathbf{1}_K$ represents a K -dimensional vector of 1's. Further, we introduce a probability distribution f supported on the positive line which is actually used to generate the edge weights. We do not specify the distribution of f . We assume that the expectation of its corresponding random variable is α_n , and the variance is larger than 0. Although we assume an community-independent weight here, we note that the results can be extended to community-independent case; see Remarks 1 and 3.

Given Θ , B , and f , the weighted network adjacency matrix $W = (W_{ij})_{1 \leq i, j \leq n}$ is generated as

$$W_{ij} = \begin{cases} \text{Bernoulli}(B_{g_i g_j}) \cdot V_{ij} & \text{if } i < j, \\ 0, & \text{if } i = j, \\ W_{ji}, & \text{if } i > j. \end{cases} \quad (2.2)$$

where $\text{Bernoulli}(p)$ denotes the bernoulli random variable which is 1 with probability p and is 0 with probability $1 - p$, V_{ij} 's denote the random variables generated from distribution f , and V_{ij} 's are mutually independent and they are also independent of $B_{g_i g_j}$'s. Define $\mathcal{W} = \alpha_n \Theta B \Theta^\top$, and it is then easy to see that \mathcal{W} is the population of W in the sense that

$\mathbb{E}(W) = \mathcal{W} - \text{diag}(\mathcal{W})$. In order to capture the higher-order connectivity patterns of the weighted network, we define the following weighted motif (triangular) adjacency matrix $W^M = (W_{ij}^M)$ to be

$$W_{ij}^M = \sum_{k=1}^n \mathbf{1}(W_{ij} \cdot W_{ik} \cdot W_{jk} > 0)(W_{ij} + W_{ik} + W_{jk}), \quad (2.3)$$

where $\mathbf{1}(\cdot)$ stands for the indicator function. Recall that in [Benson et al. \(2016\)](#); [Tsourakakis et al. \(2017\)](#), the motif (triangular) adjacency matrix was defined to be a matrix with its (i, j) 's entry being the number of triangles that nodes i and j participate in commonly. Thus (2.3) is a simple generalization of the motif adjacency matrix proposed by [Benson et al. \(2016\)](#); [Tsourakakis et al. \(2017\)](#) in order to handle the weighted networks. Now, to facilitate further analysis, let us have a closer look at the expectation of W^M . Recall (2.1) and (2.2), and then we can easily obtain the following observations. When $g_i = g_j$,

$$\mathbb{E}(W_{ij}^M) = 3\alpha_n \cdot p_n \left\{ \left(\frac{n}{K} - 2 \right) p_n^2 + (K - 1) \frac{n}{K} p_n^2 (1 - \lambda)^2 \right\} := h_1, \quad (2.4)$$

and when $g_i \neq g_j$,

$$\mathbb{E}(W_{ij}^M) = 3\alpha_n \cdot p_n (1 - \lambda) \left\{ 2 \left(\frac{n}{K} - 1 \right) p_n^2 (1 - \lambda) + (K - 2) \frac{n}{K} p_n^2 (1 - \lambda)^2 \right\} := h_2. \quad (2.5)$$

Define

$$\mathcal{W}^M = \Theta((h_1 - h_2)I_K + h_2 \mathbf{1}_K \mathbf{1}_K^\top) \Theta^\top, \quad (2.6)$$

then \mathcal{W}^M is the population of W^M by noting

$$\mathbb{E}(W^M) = \mathcal{W}^M - \text{diag}(\mathcal{W}^M).$$

Remark 1 (2.4) and (2.5) can be similarly computed under more general B 's and community-dependent weights. For example, assume that the within- and between-community probabilities are a_n and b_n , respectively, and the within- and between-community weights are α_n

and β_n , respectively, then within- and between-community expectations of W^M are

$$h_1 := a_n \left(\frac{n}{K} - 2 \right) a_n^2 \cdot 3\alpha_n + a_n (K - 1) \frac{n}{K} b_n^2 (\alpha_n + 2\beta_n),$$

$$h_2 := 2b_n \left(\frac{n}{K} - 1 \right) a_n b_n (\alpha_n + 2\beta_n) + b_n (K - 2) \frac{n}{K} b_n^2 \cdot (3\beta_n),$$

which are crucial for bounding the eigen-gap and thus the misclustering rate; see (3.4).

With these formulations at hand, we now introduce the algorithm for community detection where the goal is to recover the membership matrix Θ up to some column permutations. In this paper, we study the spectral clustering (Von Luxburg, 2007) which generally consists of two steps. The first step is to perform the eigenvalue decomposition of a suitable matrix representing the network. The next step is to run k -means on the resulting K leading eigenvectors. We consider two kinds of spectral clustering. We will mainly deal with the so-called *higher-order spectral clustering or the motif-based spectral clustering*; see Algorithm 1 for details. And we would compare it with the edge-based spectral clustering, namely, Algorithm 1 without *step 1* and with *step 2* replaced by the eigenvalue decomposition of the weighted adjacency matrix W . The goal is to study how the higher-order spectral clustering performs under the WSBM and to understand how it can enhance the clustering performance compared with that of the edge-based spectral clustering.

Remark 2 *Similar to Algorithm 1, Benson et al. (2016) and Serroux et al. (2011) also proposed spectral-based algorithms by utilizing higher-order motifs. The sweep-cut algorithm in Benson et al. (2016) essentially minimizes the motif-based conductance, which is the normalized number of motifs that are cut of two detected communities. The spectral-based algorithm in Serroux et al. (2011) approximately maximizes the motif-based modularity, which further reduces to the modularity with respect to motif adjacency matrix. In this sense, we expect that Algorithm 1 would lead to larger modularity (w.r.t. weighted motif adjacency matrix) than the edge-based counterpart does. This actually will be verified by simulated experiments in Section 5.*

The next lemma shows that \mathcal{W}^M , namely, the population version of W^M , has eigenvectors that reveal the true communities.

Lemma 1 *For a WSBM with K communities and B structured as in (2.1), suppose $\mathcal{W}^M = U\Sigma U^\top$ is the eigenvalue decomposition of \mathcal{W}^M (see 2.6), then $U = \Theta X$. Specifically, for $\Theta_{i*} = \Theta_{j*}$, we have $U_{i*} = U_{j*}$; while for $\Theta_{i*} \neq \Theta_{j*}$, we have $\|U_{i*} - U_{j*}\|_2 = \sqrt{(n_{g_i})^{-1} + (n_{g_j})^{-1}}$.*

It is easy to see from Lemma 1 that the population eigenvector has K distinct rows (n rows in total) and two rows are identical if and only if the corresponding nodes are in the same underlying community. Therefore, the higher-order spectral clustering would cluster well if the sample version eigenvectors are concentrated around its expectation. We will discuss its theoretical properties in the next section.

Algorithm 1 Higher-order spectral clustering for K communities

Input:

Community number K , a weighted adjacency matrix $W \in \mathbb{R}^{n \times n}$ representing the network;

Output:

Community membership;

- 1: **Motif matrix construction:** Construct the weighted motif adjacency matrix W^M according to (2.3).
 - 2: **Eigen-decomposition:** Find the K leading eigenvectors of W^M and form the $n \times K$ eigen-matrix.
 - 3: **k -means:** Treat each row of the eigen-matrix as a point in \mathbb{R}^K and run the Lloyd's algorithm on these points to solve k -means.
-

Table 1: A summary of the notes and notations

Notation	Definition
n	Number of nodes
K	Number of communities
Θ	Membership matrix
B	Connectivity matrix
\mathcal{W}	Population edge-based weighted adjacency matrix
\mathcal{W}^M	Population motif-based weighted adjacency matrix
W	Edge-based weighted adjacency matrix
W^M	Motif-based weighted adjacency matrix
g_i	The community which node i belongs to
G_k	Set of nodes from community k
n_k	The cardinality of G_k
p_n	The maximum link probability in \mathcal{W}
α_n	The expectation of edge weights when edge exists

3 Theoretical analysis

In this section, we theoretically justify the clustering performance of the higher-order spectral clustering under the model set-up of the WSBMs and then we compare the theoretical bounds with those of the edge-based spectral clustering.

3.1 Higher-order spectral clustering

Recall that W is the weighted adjacency matrix of a weighted graph generated from the WSBMs with n nodes and K communities (see (2.2)), and \mathcal{W} denotes the population of W . p_n is the maximum linking probability between two nodes in the WSBMs (see (2.1)) and α_n is the conditional expectation of an edge given that the edge exists. For simplicity, we assume that $W_{ij} \leq 1$ for any $1 \leq i, j \leq n$. This is reasonable since we will see in (3.8) that we require a vanishing α_n . On the other hand, one could specify the distribution of weights and using concentration inequalities to derive a $\log n$ -type bound. W^M is the corresponding weighted motif adjacency matrix (see (2.3)), where each entry is defined to

be the weighted sum of the triangles that the corresponding nodes both join, and \mathcal{W}^M denotes the population of W^M except the diagonal elements. The next theorem provides the concentration bound of the weighted motif adjacency matrix around its expectation.

Theorem 1 *Assume $p_n \geq c' \sqrt{\frac{\log n}{n}}$ for some constant $c' > 0$, and $\alpha_n p_n \geq c'' \frac{(\log n)^\beta}{n}$ for some constants $c'' > 0$ and any $0 < \beta < 1$. Let $\tau_{\max} = np_n^2$ and*

$$D = \tau_{\max}^2 n \alpha_n p_n = n^3 \alpha_n p_n^5.$$

Then for some constant $r > 0$, there exists a constant c such that with probability at least $1 - n^{-r} - \exp(-r(\log n)^\beta)$,

$$\|W^M - \mathbb{E}(W^M)\|_2 \leq c\sqrt{D}, \tag{3.1}$$

where c depends on r and β .

Remark 3 *Note that we make use of neither the structure of the connectivity matrix B nor the weights distribution to derive the results. Indeed, (3.1) holds for more general WSBMs, as long as the weights' expectations and connectivity matrix's entries are upper bounded.*

Theorem 1 requires that the network is not too sparse in the sense that $p_n \geq c' \sqrt{\frac{\log n}{n}}$ for some constant $c' > 0$, where actually ensures that the network motifs are not rare. We also require the overall signal strength is lower bounded, namely, $\alpha_n p_n \geq c'' \frac{(\log n)^\beta}{n}$ for some constants $c'' > 0$ and $0 < \beta < 1$. Theorem 1 indicates that the weighted motif adjacency matrix concentrates around its population version at the rate of $\sqrt{n^3 \alpha_n p_n^5}$. The resulting bound is similar to the Theorem 2 of Paul et al. (2018) except that α_n arises in our result. Recall that for the edge adjacency matrix, its spectral bound is the square root of the maximum expected degree (Lei and Rinaldo, 2015). Applying this law to the weighted motif adjacency matrix, its spectral bound would read as the square root of the maximum expected ‘‘motif degree’’, which is actually $\sqrt{n^2 \alpha_n p_n^3}$ as can be seen in the proof. Comparing with $\sqrt{n^2 \alpha_n p_n^3}$, the bound $\sqrt{n^3 \alpha_n p_n^5}$ in (3.1) is loose in this sense if we note that $p_n \geq c' \sqrt{\frac{\log n}{n}}$ for some constant $c' > 0$.

Now we are ready to study the clustering performance of the higher-order spectral clustering. Specifically, we use the following metric to evaluate the quality of clustering,

$$L(\hat{\Theta}, \Theta) = \min_{J \in E_K} \sum_{1 \leq k \leq K} (2n_k)^{-1} \|(\hat{\Theta}J)_{G_{k*}} - \Theta_{G_{k*}}\|_0, \quad (3.2)$$

where $\hat{\Theta}$ denotes the estimated membership matrix by the higher-order spectral clustering, and E_K denotes the set of all $K \times K$ permutation matrices. Obviously, L measures the sum of the fractions of the misclustered nodes within each community. The following theorem provides an upper bound on L .

Theorem 2 *Let $\hat{\Theta}$ be the estimated membership matrix by the higher-order spectral clustering, and denote the minimum non-zero eigenvalue of \mathcal{W}^M as $\lambda_K(\mathcal{W}^M)$. Suppose the assumptions in Theorem 1 hold, and there exists a constant $c > 0$ such that, if*

$$\frac{K^3}{n\alpha_n p_n} \leq 1/c, \quad (3.3)$$

then with probability at least $1 - n^{-r} - \exp(-r(\log n)^\beta)$ for some constant $r > 0$ and any $0 < \beta < 1$, there exist subsets $S_k \subseteq G_k$ for $k = 1, \dots, K$ such that

$$L(\hat{\Theta}, \Theta) \leq \sum_{k=1}^K \frac{|S_k|}{n_k} \leq c \frac{K \|W^M - \mathcal{W}^M\|_2^2}{\lambda_K^2(\mathcal{W}^M)} \leq c \frac{K^3}{n\alpha_n p_n}. \quad (3.4)$$

Moreover, for $G = \cup_{k=1}^K (G_k \setminus S_k)$, there exists a $K \times K$ permutation matrix J such that

$$\hat{\Theta}_{G_*} J = \Theta_{G_*}, \quad (3.5)$$

where we recall that $\hat{\Theta}_{G_}$ and Θ_{G_*} denote the submatrix of $\hat{\Theta}$ and Θ consisting of the rows indexed by G .*

Theorem 2 indicates that the misclustering rate of the motif-based spectral clustering is bounded by $O(\frac{K^3}{n\alpha_n p_n})$ with high probability. (3.3) is a technical condition that provides the range of parameters (K, n, α_n, p_n) under which the conclusions hold. S_k in (3.4) is

actually the set of misclustered nodes in the true community G_k . The result in (3.4) is high-dimensional in that each parameter can vary with the number of nodes n . The bound vanishes under several parameter settings. For example, when $\alpha_n \asymp \log n/n$ and $p_n \asymp 1/(\log n)^{1-\beta}$ where $\beta \in (0, 1)$ and $f(n) \asymp g(n)$ if $cg(n) \leq f(n) \leq Cg(n)$ for some constants $0 < c < C < \infty$, then $K = o((\log n)^{\beta/3})$ ensures a vanishing misclustering bound.

3.2 Comparison with edge-based spectral clustering

To understand how the higher-order spectral clustering enhances the misclustering performance, we compare its misclustering bounds with those from edge-based spectral clustering. Note that edge-based spectral clustering has been studied by [Lei and Rinaldo \(2015\)](#); [Rohe et al. \(2011\)](#) under the *unweighted* SBMs. One can easily modify the proofs in [Lei and Rinaldo \(2015\)](#) to obtain the corresponding results under the WSBMs, hence we omit the details. It is easy to learn from [Theorem 2](#) that the spectral bound ($\|A - \mathcal{A}\|_2$) and the minimum non-zero eigenvalue of the population input matrix ($\lambda_K(\mathcal{A})$) have the following relationship with the misclustering rate L defined in (3.2),

$$L \leq c \frac{K \|A - \mathcal{A}\|_2^2}{\lambda_K(\mathcal{A})^2}, \quad (3.6)$$

where c is some constant, A can be W or W^M , and \mathcal{A} can be \mathcal{W} or \mathcal{W}^M correspondingly. Hence, we list these three metrics of the two spectral clustering methods in [Table 2](#). The bounds in [Table 2](#) show that when

$$\frac{cK^3}{n\alpha_n p_n} \leq \frac{c''K^3 \log n}{n^2 \alpha_n^2 p_n^2}, \quad (3.7)$$

the higher-order spectral clustering has a lower misclustering rate than does the edge-based counterpart. Combining (3.7) with the parameter assumption in [Theorem 1](#) leads to the

following parameter ranges

$$\begin{cases} \alpha_n \leq c \frac{\log n}{n} / p_n, \\ p_n \geq c' \sqrt{\frac{\log n}{n}}, \\ \alpha_n p_n \geq c'' \frac{(\log n)^\beta}{n}, \end{cases} \quad (3.8)$$

which can be all met when, for example, $\alpha_n \asymp \log n/n$ and $p_n \asymp 1/(\log n)^{1-\beta}$, where $\beta \in (0, 1)$ is any constant that arises in Theorem 1. The first inequality in (3.8) requires that the signal strength is weak if we notice the second inequality. The second inequality says that the network density should be large at a certain level. And the third inequality could be thought of as a requirement of the overall signal strength of weight and network density. As a result, when the network is dense with a weak signal of weights, the higher-order spectral clustering can be better than its edge-based counterpart in terms of the clustering error. In addition, although we only specify the expectation of conditional weights, we implicitly assume that the variance of weight is larger than 0. In fact, the unweighted SBMs can not lead to the advantage of the higher-order spectral clustering over the edge-based counterpart, which is consistent with the results in Paul et al. (2018) (see Section 3.5 in Paul et al. (2018)).

Remark 4 *It is worth noting that there exists statistical minimax misclustering error rate under SBMs and a general weighted SBMs (Gao et al., 2017; Xu et al., 2020). However, we here focus on enhancing the clustering performance of the spectral clustering by using the weighted motif adjacency matrix. We show that the higher-order spectral clustering leads to a lower misclustering upper bound if the network is dense with a weak expected signal of weights, which is partially because the motif-based adjacency matrix enlarges the eigen-gap between the smallest non-zero eigenvalue and 0 of the population matrix (see Table 2). Similar observations are obtained in Wang et al. (2018), and our empirical results in Section 5 also validate the theoretical results. It is left as future work to compare these two spectral clustering methods more delicately, for example, deriving tighter bounds or studying the strong consistency of both methods.*

Table 2: A summary of the main results of two spectral clustering methods under the WSBMs.

Bounds	Edge-based	Motif-based
Spectral bound	$O_p(\sqrt{\max\{n\alpha_n p_n, c\log n\}})$	$O_p(\sqrt{n^3 \alpha_n p_n^5})$
λ_K	$O(\frac{n\alpha_n p_n}{K})$	$O(\frac{n^2 \alpha_n p_n^3}{K})$
misclustering rate	$O_p(\max\{\frac{K^3}{n\alpha_n p_n}, \frac{K^3 \log n}{n^2 \alpha_n^2 p_n^2}\})$	$O_p(\frac{K^3}{n\alpha_n p_n})$

4 Discussions

In this section, we discuss our work from methodology to theory. Possible extensions are also posed.

Methodology. Conceptually, although we focused on the spectral clustering, the notion of motif adjacency matrix could be used as the input of many community detection methods. From this point of view, it can be regarded as a data preprocessing technique. [Qin and Rohe \(2013\)](#) showed that the regularized graph Laplacian in which the degree matrix is regularized with a small constant can lead to better clustering results than the original spectral clustering. Similarly, using the motif adjacency matrix instead of the adjacency matrix can be thought of as one network denoising technique.

On the other hand, driven by the evidence that network edges often contain sensitive information, there is a growing body of works on the privacy-preserving analysis of networks; see [Karwa and Slavković \(2016\)](#); [Karwa et al. \(2017\)](#), among others. From this perspective, the entries of the motif adjacency matrix can be regarded as the summary statistics, and thus it can help protect the original edges to some extent.

Computationally, there is no doubt that counting the number of triangles for each pair of nodes is costly on large-scale networks. One could use sampling techniques to improve the computational performance ([Seshadhri et al., 2014](#); [Benson et al., 2016](#); [Chen and Chen, 2018](#); [Guo et al., 2020](#); [Zhang et al., 2022](#)).

Theory. Theorem 1 and Theorem 2 are our main results. Theorem 1 investigates the deviation of the weighted motif adjacency matrix from its population version in the sense of the spectral norm. We generally use the ϵ -net technique to make a discretization, and then use a combinatorial method to bound the approximation error. This technique was first developed by Feige and Ofek (2005). Since that time it has been widely used by statistics and machine learning communities; see Lei and Rinaldo (2015); Paul et al. (2018); Gao et al. (2017); Chin et al. (2015), among many others. Note that the entries of W^M are dependent which creates difficulty in deriving the bound. To tackle this issue, we use similar arguments developed in Paul et al. (2018). In particular, we make use of the *typical bounded difference inequality* established in Warnke (2016) to handle the dependency. Note that as the network edges in our model are not Bernoulli distributed and the resulting weighted motif adjacency matrix is not identical to theirs, the details of our proof are slightly different from Paul et al. (2018). It remains unclear whether the bound in (3.1) could be improved by using other techniques. Theorem 2 bounds the misclustering rate of the motif-based spectral clustering. The general idea is to use the Davis-Kahan theorem (Davis and Kahan, 1970) to bound the perturbation of eigenvectors from the approximation error bound (3.1). Such framework is widely used in Lei and Rinaldo (2015); Rohe et al. (2011), among others.

Extensions. We mainly study the full rank WSBMs, that is, the rank of \mathcal{W} equals the target community number K . Actually, all the results could be generalized to rank-deficient WSBMs (i.e., $\text{rank}(\mathcal{W}) \leq K$) by investigating the population eigen-structure of such WSBMs and adding extra conditions on B , just as the argument in Zhang et al. (2022). In addition, though we mainly deal with the clustering performance, we can estimate the connectivity matrix $B = (B_{ql})_{q,l=1,\dots,K}$ via the following simple plug-in estimator,

$$\hat{B}_{ql} := \frac{\sum_{1 \leq i, j \leq n} W_{ij}^M \hat{\Theta}_{iq} \hat{\Theta}_{jl}}{\sum_{1 \leq i, j \leq n} \hat{\Theta}_{iq} \hat{\Theta}_{jl}}, \quad 1 \leq q, l \leq K.$$

Moreover, we could evaluate its theoretical performance by using Theorem 1 and 2. Following the advantage of motif-based spectral clustering in terms of clustering, we can imagine that the motif-based method would lead to better estimates of B than the edge-based

method does. For the sake of space, we leave all these extensions as our future work.

5 Simulation studies

In this section, we empirically compare the finite sample performance of the higher-order spectral clustering, namely, the motif-based spectral clustering (denoted by *motif-based*) with that of the edge-based spectral clustering (denoted by *edge-based*) under the WS-BMs. Note that we use higher-order spectral clustering and motif-based spectral clustering interchangeably in this section. To that end, we first carry out a sensitivity analysis to evaluate our theoretical findings. Then, we provide several extended experiments to show that high-order spectral clustering has an advantage under a broad regime even when some theoretical assumptions are violated.

First, we evaluate the performance of two methods and validate the theoretical results. To be consistent with Section 3, we use the following three metrics to assess the performance of each method. The first is the spectral deviation of the weighted motif adjacency matrix W^M from its population version \mathcal{W}^M , denoted by *spectral bound*. The second is the minimum non-zero eigenvalue of the population \mathcal{W}^M , denoted by *eigen gap*. The third is the summation of the ratio of misclustered nodes within each true community (see (3.2)), denoted by *misclustering rate*. We study the effect of sample size n , the effect of maximum link probability p , the effect of out-in-ratio (the ratio of the between-community probability q over the within-community probability p), and the effect of the number of communities K respectively with the following experimental set-ups,

- *Effect of n* : $K = 2, p = 0.5, q = p(1 - 0.4)$, and n varies;
- *Effect of p* : $K = 2, n = 60, q = p(1 - 0.4)$, and p varies;
- *Effect of out-in-ratio*: $K = 2, n = 60, p = 0.5$, and $\frac{q}{p}$ varies;
- *Effect of K* : $n = 120, p = 0.5, q = p(1 - 0.4)$, and K varies;

where the weights are all *i.i.d.* generated from uniform distribution $\text{Uniform}(0.01, 1)$ provided that there is an edge.

Figures 1-4 show the results for the above four experimental set-ups. As indicated in Section 3, the spectral bound and the eigen-gap with respect to the two spectral clustering methods have different scales. Hence we use two axes to show their tendency. Specifically, the left and right axes correspond to motif-based and edge-based spectral clustering, respectively. The numerical results show satisfactory consistency with the theoretical results. For the spectral bound, the motif-based spectral clustering grows super-linearly with n and p , while the edge-based spectral clustering grows sub-linearly with n and p (see Figures 1(a) and 2(a)). Note that we have not taken the community structure into consideration when bounding the spectral error. While as indicated in Figures 3(a) and 4(a), the spectral bounds grow with the increasing of out-in-ratio and drop with the increasing number of communities. Hence, it would be beneficial to incorporate this information when bounding the spectral error. We leave this for our future work. For the eigen-gap, as n and p increase, the motif-based spectral clustering grows faster than the edge-based spectral clustering does, where the latter has linear growth with n and p (see Figures 1(b) and 2(b)). In addition, the eigen-gap decreases with the growth of K for both methods. As for the misclustering rate, we can see from Figures 1(c), 3(c), and 4(c) that when n , out-in-ratio, and K are intermediate, the motif-based spectral clustering has great advantage over the edge-based method in clustering. When these terms are too small or too large, the signal for the communities is weak such that neither method can recover the communities, or the signal is strong such that the edge-based clustering can do well. In particular, we see from Figure 2(c) that when the network is sparse, the edge-based spectral clustering is better than the motif-based method. As the maximum linking probability p increases, the motif-based spectral clustering performs gradually better than the edge-based method does. This is consistent with our theoretical findings.

Next, we provide additional experiments to show that motif-based spectral clustering has the advantage in wide scenarios where the theoretical requirements are not necessarily met. We use Adjusted Rand Index (ARI) (Manning et al., 2010), Normalized Mutual Information (NMI) (Manning et al., 2010), and Modularity (Newman, 2006) to justify the clustering performance of the two methods, where larger scores indicate better cluster-

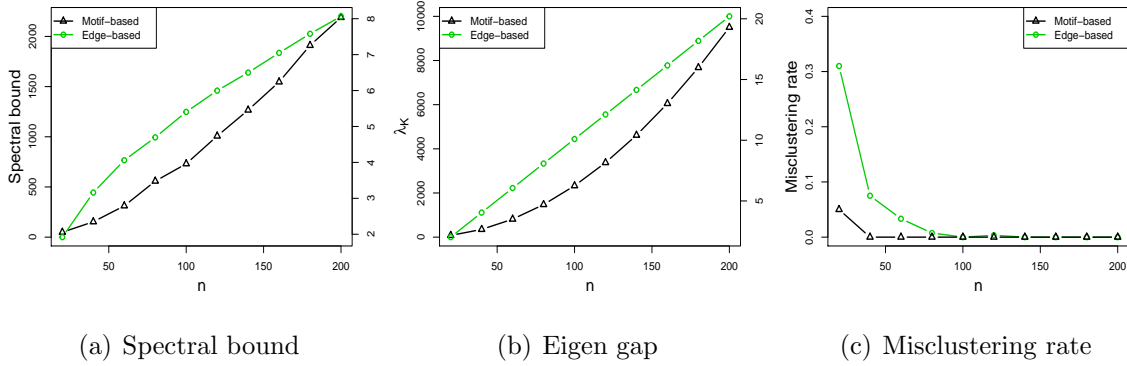


Figure 1: The average effect of n on the three metrics over 100 replications. Other parameters $K = 2, p = 0.5, q = p(1 - 0.4)$, and the edge weights are *i.i.d.* generated from Uniform(0.01, 1) provided that the edges exist. In (a) and (b), the left and right axes correspond to motif-based and edge-based spectral clustering, respectively.

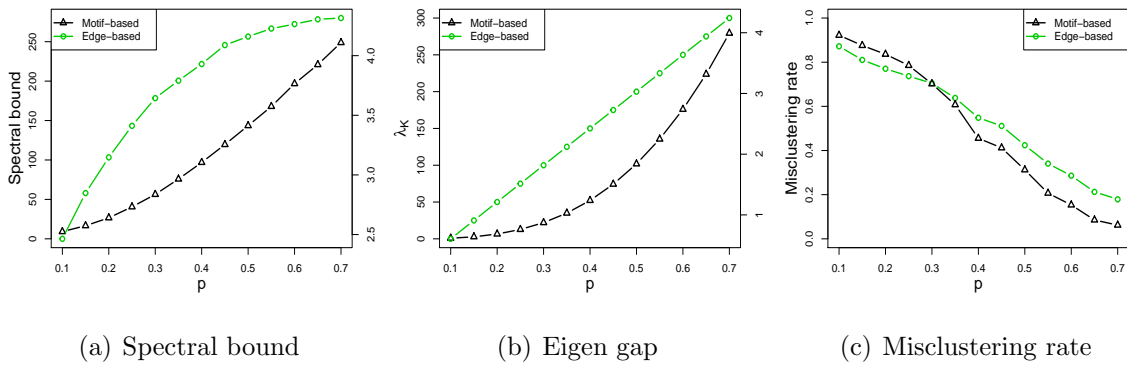


Figure 2: The average effect of p on the three metrics over 100 replications. Other parameters $K = 2, n = 60, q = p(1 - 0.4)$, and the edge weights are *i.i.d.* generated from Uniform(0.01, 1) provided that the edges exist. In (a) and (b), the left and right axes correspond to motif-based and edge-based spectral clustering, respectively.

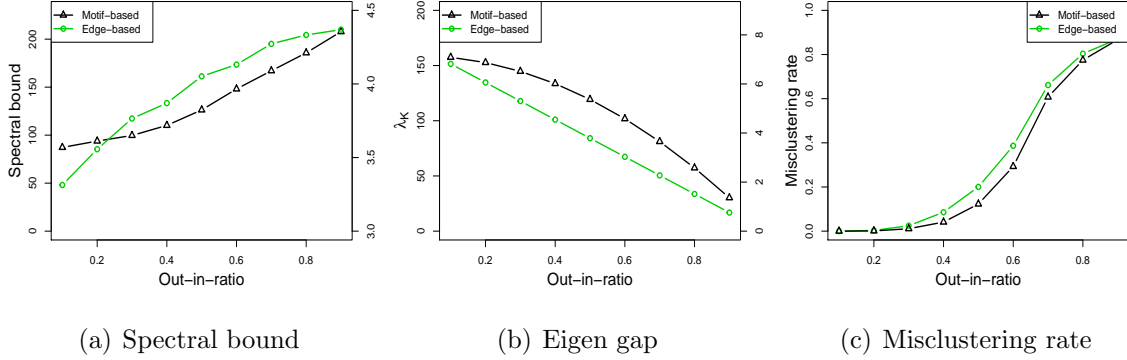


Figure 3: The average effect of out-in-ratio on the three metrics over 100 replications. Other parameters $K = 2, n = 60, p = 0.5$, and the edge weights are *i.i.d.* generated from $\text{Uniform}(0.01, 1)$ provided that the edges exist. In (a) and (b), the left and right axes correspond to motif-based and edge-based spectral clustering, respectively.

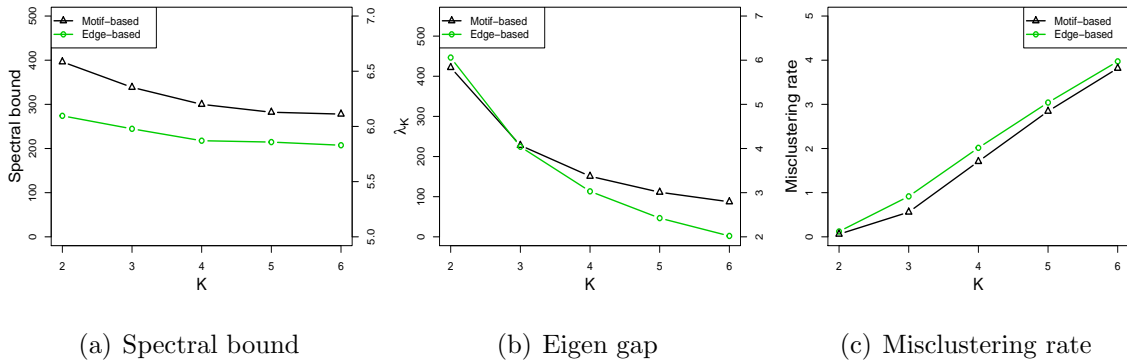


Figure 4: The average effect of K on the three metrics over 100 replications. Other parameters $n = 120, p = 0.5, q = p(1 - 0.4)$, and the edge weights are *i.i.d.* generated from $\text{Uniform}(0.01, 1)$ provided that the edges exist. In (a) and (b), the left and right axes correspond to motif-based and edge-based spectral clustering, respectively.

ing performance. In particular, ARI and NMI are computed by comparing the estimated communities of each of the methods with the true underlying communities in SBMs, respectively. Modularity is computed based on the *weighted motif adjacency matrix*, which measures the difference between the strength of edges (i.e., the weighted edges in the weighted motif adjacency matrix) between any two nodes in the same community and the expected strength of edges between them. As explained in Remark 2, we expect that motif-based spectral clustering would lead to larger modularity. In particular, we conduct the following experiments.

Core-periphery structure. The previous experiments focused on recovering the *affinity* structure in networks. That is, the two communities have relatively high within-community link probability compared to the between-community link probability. We here assume that the network exhibit *core-periphery* structure, that is, one of the two communities has a relatively high within-community link probability compared to both the other cluster’s within-community link probability and the between-community link probability (Pribe et al., 2019). Specifically, we assume the connectivity matrix $B := [0.5, 0.3; 0.3; 0.05]$ and let the sample size n vary. Figure 5 shows that in our set-up, the motif-based method has the advantage over the edge-based counterpart in terms of all three metrics, which corroborates the ability of the motif-based method for finding core-periphery structure (Benson et al., 2016).

Disassortative weights. In theoretical analysis, we assumed that all the weights are *i.i.d.* regardless of the communities. We assume that the weights are *disassortative* in that the within-community edges have less weight than the between-community edges. In particular, the between-community weights are *i.i.d.* Uniform(0.5, 1), and the within-community weights are *i.i.d.* Uniform(0.01, 0.5). While the communities are *assortative* in that the within-community edges have a larger link probability than between-community edges. It is obvious that this structure brings difficulty to the estimation of communities.

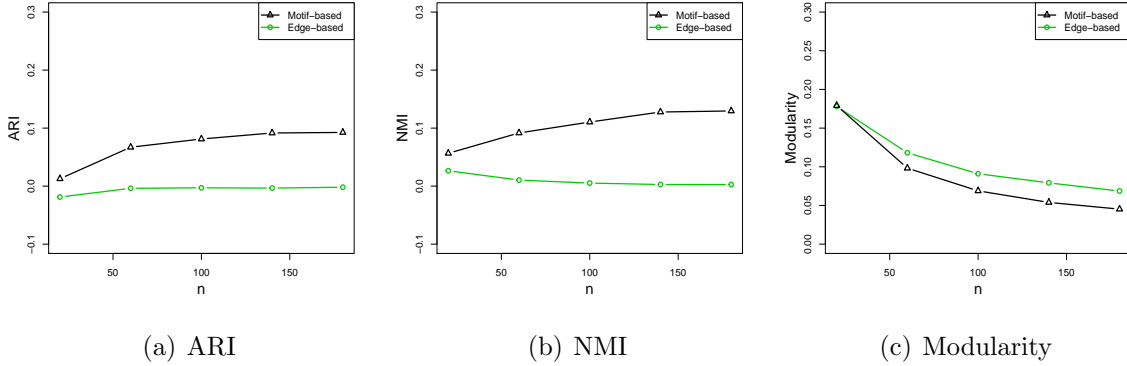


Figure 5: The average performance of two methods on networks with core-periphery structure over 100 replications. The parameters are $B := [0.5, 0.3; 0.3; 0.05]$, $K = 2, n = 60$. The weights are *i.i.d.* generated from $\text{Uniform}(0.5, 0.6)$ provided that the edges exist.

Figure 6 shows that the motif-based method remains to be better than the edge-based method in this regime. It is worth mentioning that when the weights and communities are both assortative, the edge-based method is good enough to recover the communities since the signal is strong enough then.

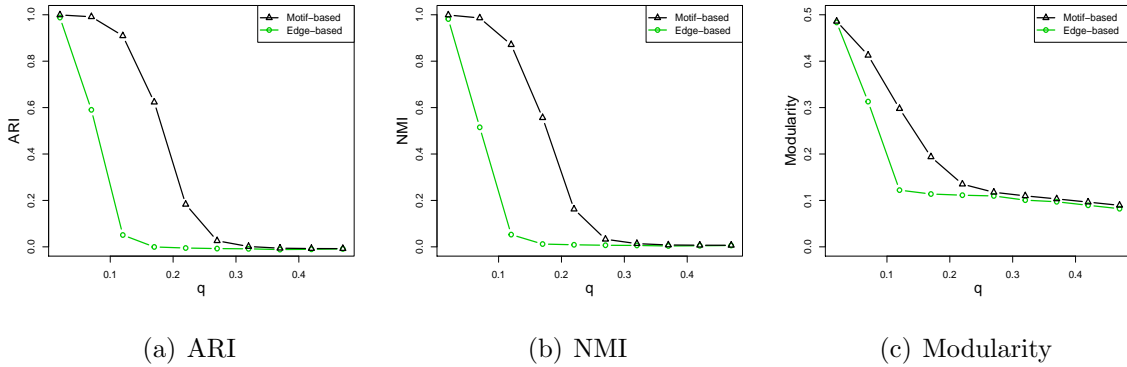
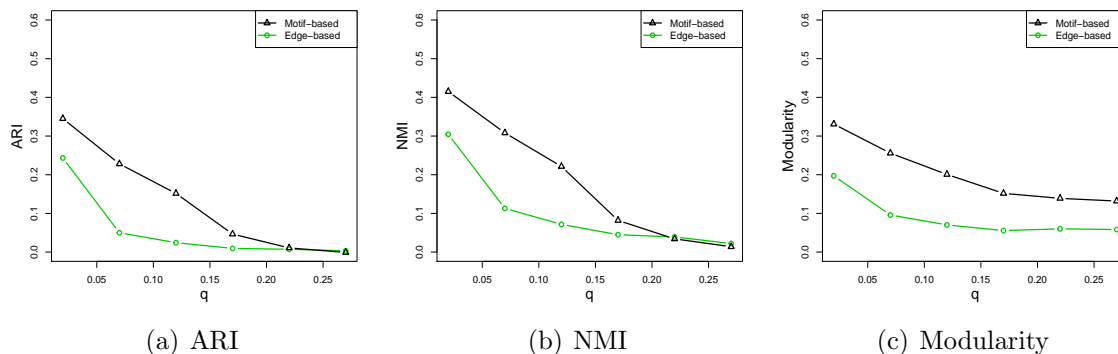


Figure 6: The average performance of two methods on networks with disassortative weights over 100 replications. The parameters are $K = 2, n = 60, p = 0.5$. The between-community weights are *i.i.d.* $\text{Uniform}(0.5, 1)$, and the within-community weights are *i.i.d.* $\text{Uniform}(0.01, 0.5)$.

Other weight distributions. The aforementioned experiments involved uniformly dis-

tributed network weights. Here, we test the efficacy of the motif-based method on two other distributions. The first is the chi-squared distribution with degree of freedom 1, denoted by $\chi^2(1)$. The second is the exponential distribution with mean 1, denoted by $\exp(1)$. The corresponding results are shown in Figure 7. It can be seen that the motif-based spectral clustering performs better than the edge-based counterpart, which shows that the efficacy of the motif-based method is not restrictive in terms of the distribution of weights.

(I) Weights from $\chi^2(1)$



(II) Weights from $\exp(1)$

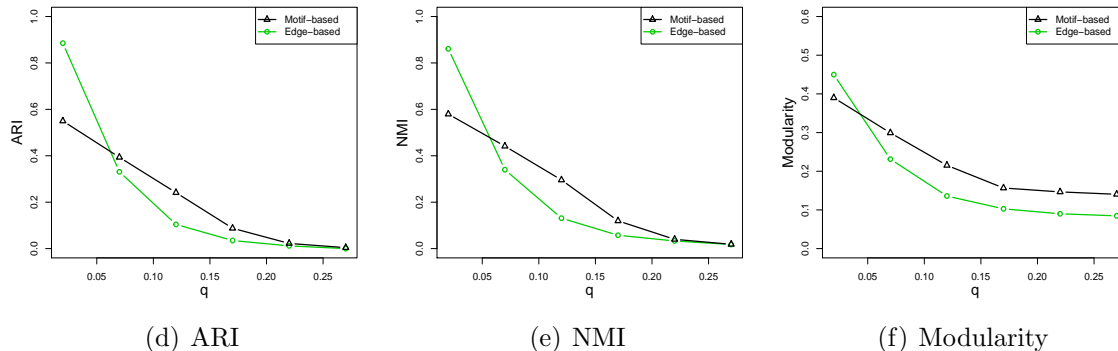
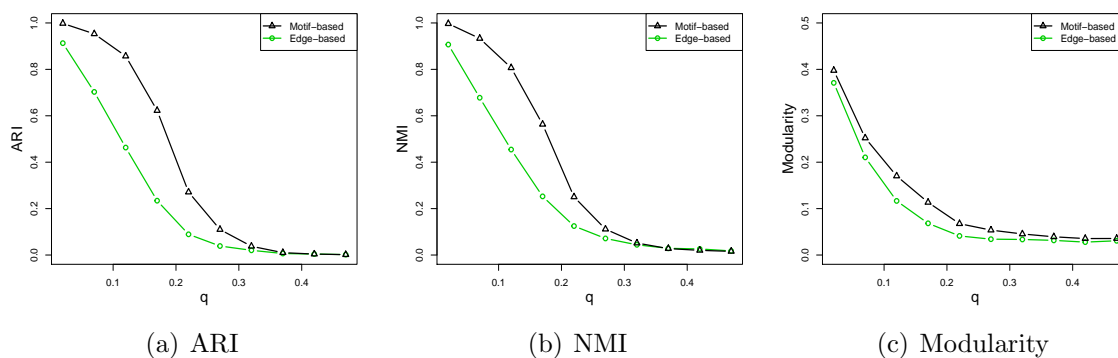


Figure 7: The average performance of two methods on networks with two kinds of weight distributions. (I) and (II) correspond to the results with the network weights *i.i.d.* generated from $\chi^2(1)$ and $\exp(1)$, respectively. Other parameters are $n = 60, p = 0.3, K = 2$.

Other motifs. From both the theoretical and algorithmic sides, we have mainly focused on the triangular motif in motif-based spectral clustering. It is of interest to see whether

motif-based spectral clustering remains powerful on other motifs. We here test the algorithm on two other motifs. The first is the wedge motif, which is the subgraph with three nodes and two edges. The second is the four-nodes clique motif, which is the totally connected subgraph with four nodes and six edges. The weighted motif adjacency matrix is then formulated by adding the weights in the motif that the node pairs participate in. Figure 8 shows the results. It turns out that motif-based spectral clustering is also effective on these two motifs. Hence, it would be interesting to theoretically study the consistency.

(I) Wedge motif



(II) Four-nodes clique

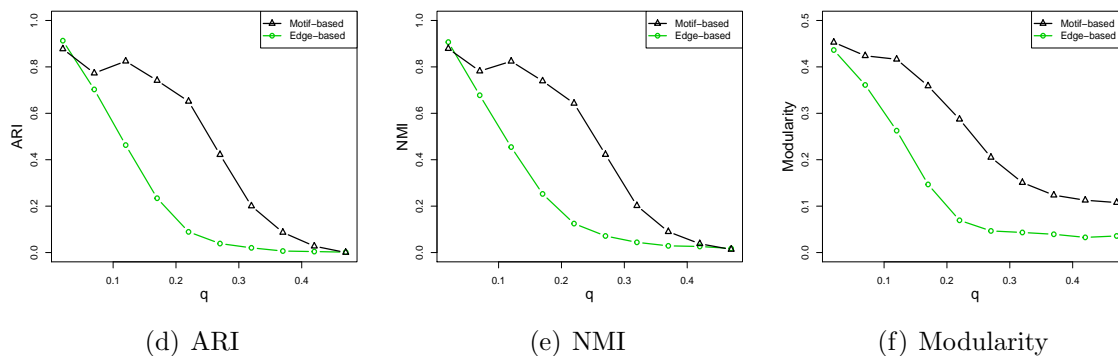


Figure 8: The performance of two methods, where the motif-based spectral clustering is based on (I) the wedge motif and (II) the four-nodes clique, respectively. The parameters are $K = 2, n = 60, p = 0.5$, and the edge weights are *i.i.d.* $\chi^2(1)$.

To sum up, the above experiments show that the motif-based spectral clustering has the advantage over the edge-based counterpart when the clustering problem is relatively hard, namely, the signal of communities is weak. And the applicable range of motif-based

spectral clustering is far beyond the limits of theory. It is also worth noting that by our simulated examples, the modularity is a good measure to judge between the two methods when the true clustering labels are not known.

6 Real data analysis

In this section, we show the merits of higher-order spectral clustering using three real datasets, including the statisticians' citation network, statisticians' coauthor network, and the PM_{2.5} data set. In the sequel, we introduce the datasets and their corresponding clustering results, respectively. To save space, all the clustering results are included in the Supplementary Material.

Statisticians citation network. This dataset was initially collected by [Ji and Jin \(2016\)](#) based on all published papers from 2003 to the first half of 2012 in four of the top statistical journal: *Annals of Statistics*, *Biometrika*, *Journal of American Statistical Association* and *Journal of Royal Statistical Society (Series B)*, which results in 3248 papers and 3607 authors in total. We here study a citation network, where each node represents an author and the number of edges between any pair of nodes is equal to the number of one-way citations between the two authors. We consider the largest connected components of this network which includes 2654 nodes. We set $K = 3$ as in [Ji and Jin \(2016\)](#). [Figure 10](#) and [11](#) shows the clustering results for the higher-order and the edge-based spectral clustering, respectively. We can see from [Figure 10\(a\)](#) and [11\(a\)](#) that both of the two methods find two small communities and one large community, which can be regarded as the background community. Hence, we take a closer look at the two small communities. As shown in [Figure 10\(b\)](#) and [10\(c\)](#), the motif-based spectral clustering detects two communities with many triangles. One community (see [Figure 10\(b\)](#)) consists of statisticians in high-dimensional statistics, including but without limiting to the authors of the lasso, group lasso, adaptive lasso, SCAD, graphical models, which are pioneering works of high-dimensional statistics in the past 20 years. The other community ([10\(c\)](#)) consists of 5 statisticians engaged in a functional analysis or non-parametric statistics. Turning to the edge-based spectral clustering, we find that one community (see [Figure 11\(c\)](#)) includes

7 statisticians engaged in functional analysis and non-parametric statistics, which is very similar to the non-parametric statistics community found by the motif-based clustering because only two more statisticians are included. After examining the other community (see Figure 11(b)) carefully, we find that this community is comprised of two statistician communities, namely, high-dimensional statisticians and Bayesian statisticians, and statistician Michael Jordan bridges these two communities. The results are quite interesting, but from the clustering point of view, motif-based spectral clustering leads to better results since the resulting communities are purer.

Statisticians coauthor network. This network was also generated based on the aforementioned dataset (Ji and Jin, 2016). In particular, each node represents an author and the number of edges between any pair of nodes equals to the number of papers they coauthored. We consider the largest connected components of the network which result in 2263 nodes. We also set $K = 3$ as in Ji and Jin (2016). Figure 12 and 13 display the clustering results for the motif-based and edge-based spectral clustering, respectively. We can see clearly that both methods detect two main communities, and the remaining communities are so large that we regard them as the background. In particular, the motif-based spectral clustering detected two communities (see Figure 12(b) and 12(c)), which include statisticians engaged in biostatistics/medical statistics and Bayesian statistics, respectively. By contrast, the edge-based spectral clustering detects one community (see Figure 13(b)) with 3 biostatisticians who have worked or studied at Harvard. And the other community (see Figure 13(c)) includes two disconnected components, where one consists of statisticians in biostatistics/medical statistics, and the other includes statisticians in non-parametric statistics. Hence, motif-based spectral clustering detects more reasonable communities than edge-based ones.

PM_{2.5} pollution data. We collected the PM_{2.5} data which consists of daily averaged PM_{2.5} concentration in the year 2015 for each of the 31 Chinese capital cities. In more detail, for each city, we have its daily averaged PM_{2.5} concentrations for 354 days except 11 days containing missing data. We aim to study the communities of cities in terms of the PM_{2.5} pollution. For this purpose, we should construct the PM_{2.5} pollution network

first. Graphical models provide a useful tool for constructing the network from such data. Specifically, we treat the $\text{PM}_{2.5}$ concentration of each city as a random variable (i.e., the node in the resulting network) and employ the graphical lasso (Yuan and Lin, 2007; Friedman et al., 2008) with the tuning parameter selected by eBIC (Foygel and Drton, 2010) to obtain a weighted network, whereby the rationality of graphical models, the absolute weight between any pair of nodes (cities) is proportional to the conditional correlation of the two corresponding random variables, given the remaining variables. We set $K = 5$, which is consistent with the output by the fast greedy modularity optimization algorithm (Clauset et al., 2004) that decides the number of communities automatically. Figure 14 and 15 show the clustering results corresponding to the motif-based and the edge-based spectral clustering, where for ease of interpretation, we show the cities on the Chinese map. It can be seen from Figure 14 and 15 that, both methods detect communities of cities such that cities within each community are closely located. It could be explained by the fact that the cities located closely share similar meteorological, economic, and industrial patterns, thus leading to the conditional dependence of their $\text{PM}_{2.5}$ pollution. However, the communities detected by the two methods are different in some sense. There are two main differences. The first difference is that two communities detected by the motif-based method in Figure 14(c) and 14(f) are generally merged into one single community (see Figure 15(e)) by the edge-based method. The second difference is that the community found by the motif-based method in Figure 14(d) is generally divided into two communities by the edge-based method (see Figure 15(d) and 15(f)). One who has common sense about Chinese geography will feel that the communities detected by the motif-based method are more reasonable. As an explanation, we conduct a two-sample t-test to test whether the average $\text{PM}_{2.5}$ value of cities within the two communities in Figure 14(c) and 14(f) (motif-based communities) have a significant difference. The answer is yes, with the p-value smaller than 2.2×10^{-16} . Similarly, we also test the difference between the two communities in Figure 15(d) and 15(f) (edge-based communities) in terms of the mean for $\text{PM}_{2.5}$. Whereas the answer is no, with the p-value being 0.819. The above analysis indicates that the motif-based method yields more reasonable communities than the edge-based method does.

Comparison of modularity. The aforementioned analysis shows that the motif-based spectral clustering can yield more interpretable communities than the edge-based counterpart, which is consistent with the results in [Benson et al. \(2016\)](#). As a complement, we also compute the modularity of the communities obtained by both methods; see [Section 5](#) for details of modularity. [Figure 9](#) displays the box plot of the modularity of two methods on three datasets over 100 replications. It turns out that the motif-based method has slightly larger modularity than the edge-based counterpart on the latter two datasets. While it is slightly worse than the edge-based one on the first dataset. In addition, it is obvious that the motif-based method is far more stable than the edge-based method, which makes the motif-based method more desirable in real applications.

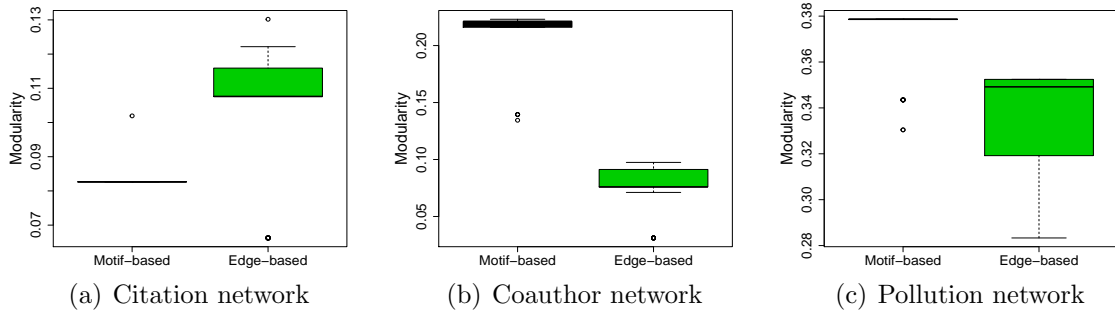


Figure 9: The box plot of modularity of two methods on three datasets over 100 replications. The modularity is computed based on the weighted motif adjacency matrix.

7 Conclusion

The higher-order structure of networks and the corresponding higher-order spectral clustering have been proven to be insightful and helpful in real network clustering problems. However, there are rare works disclosing the merits of higher-order spectral clustering over the edge-based one systematically and theoretically. Motivated by this, we theoretically studied the clustering performance of the higher-order spectral clustering from a statistical perspective, where we typically assumed the underlying networks are generated from

a weighted stochastic block model. The results showed that when the network is dense and the signal of weights is weak, the higher-order spectral clustering could produce better misclustering upper bound than the edge-based counterpart. The methodologies and theories in this paper can be generally used in other problems. For example, the weighted motif adjacency matrix can be thought of as a network denoising trick and can be used for any downstream network analysis. In addition, the theoretical tools in this paper can be used to analyze networks with summary statistics but without edge information, which is of independent interest in the context of privacy-preserving network analysis.

There are many ways that the content of this work could be extended. First, we only specify the expectation of weights in the WSBM. It would be beneficial to derive more delicate results if the distribution of weights is incorporated. Second, we found by experiments that higher-order spectral clustering also works better than edge-based under the degree-corrected stochastic block models. It would be interesting to understand this phenomenon theoretically, which is currently under our consideration. Third, we considered triangles in undirected networks. More types of higher-order motifs and the clustering in directed networks deserve further research. Besides, it is of interest to see whether the motif-based method can be generalized to the clustering of multi-layer networks (Paul and Chen, 2020). Finally, we take a step forward in understanding how higher-order spectral clustering works, and there is still an urgent need to understand it thoroughly. In addition, it is crucial to develop a network-generating model that really captures the higher-order connectivity patterns in real networks.

Acknowledgement

This work is partially done when Xiao Guo was a visiting student at Columbia University. The authors would like to thank Professor Ming Yuan for enlightening discussions in the early stage of this project. Our research is partially supported by National Natural Science Foundation for Outstanding Young Scholars (No.72122018), National Natural Science Foundation of China (No.U1811461), and Natural Science Foundation of Shaanxi Province (No. 2021JQ-429 and No.2021JC-01).

SUPPLEMENTARY MATERIAL

This file includes the proofs for theorems and the figures on clustering results of real data analysis.

A. Proof of main results

Proof of Lemma 1

Let $\Delta = \text{diag}(\sqrt{n_1}, \dots, \sqrt{n_K})$ and recall (2.6), then we have

$$\begin{aligned} \mathcal{W}^M &= \Theta((h_1 - h_2)I_K + h_2\mathbf{1}_K\mathbf{1}_K^\top)\Theta^\top \\ &= \Theta\Delta^{-1}\Delta((h_1 - h_2)I_K + h_2\mathbf{1}_K\mathbf{1}_K^\top)\Delta(\Theta\Delta^{-1})^\top, \end{aligned}$$

where $h_1 > h_2 > 0$. Recalling the structure of Θ , one can easily show $\Theta\Delta^{-1}$ is orthonormal. Denote the eigen-decomposition of $\Delta((h_1 - h_2)I_K + h_2\mathbf{1}_K\mathbf{1}_K^\top)\Delta$ as

$$Z\Sigma Z^\top = \Delta((h_1 - h_2)I_K + h_2\mathbf{1}_K\mathbf{1}_K^\top)\Delta.$$

Then we have

$$\mathcal{W}^M = \Theta\Delta^{-1}Z\Sigma(\Theta\Delta^{-1}Z)^\top = U\Sigma U^\top.$$

Thus $U = \Theta\Delta^{-1}Z = \Theta X$ with $X := \Delta^{-1}Z$ as $\Theta\Delta^{-1}$ and Z are orthonormal, respectively. Moreover, as Z is orthonormal and $\Delta^{-1}Z$ is a square matrix, we can verify that the rows of $\Delta^{-1}Z$ are perpendicular to each other and the k th row has length $\sqrt{1/n_k}$, which implies $\|X_{k*} - X_{l*}\|_2 = \sqrt{n_k^{-1} + n_l^{-1}}$. ■

Proof of Theorem 1

The general framework of the following proof is adapted from Feige and Ofek (2005), whose arguments are also used in Lei and Rinaldo (2015); Paul et al. (2018); Chin et al. (2015); Gao et al. (2017), among others. The proof includes three major steps.

Step 1: Discretization. We first reduce controlling $\|W^M - \mathbb{E}(W^M)\|_2$ to the problem of bounding the supremum of $|x^\top(W^M - \mathbb{E}(W^M))y|$ over all pairs of vectors x, y in a finite set of grid points. For any given pair (x, y) in the grid, the quantity $x^\top(W^M - \mathbb{E}(W^M))y$ is decomposed into the sum of two parts. The first part corresponds to the small entries of both x and y , called the *light pairs*, the other part corresponds to large entries of x or y , called the *heavy pairs*.

Step 2: Bounding the light pairs. Since the elements of W^M are dependent, we can not use the Bernstein's inequality to control the contribution of the light pairs. Instead, we make use of the typical bounded differences inequality established in [Warnke \(2016\)](#) to bound the light pairs. Note that [Paul et al. \(2018\)](#) also used similar arguments to do this in the unweighted SBMs, but the details are different from those we do in the weighted case.

Step 3: Bounding the heavy pairs. The contribution from heavy pairs will be bounded using a combinatorial argument on the event that the edge weights (w.r.t. the weighted motif adjacency matrix W^M) in a collection of subgraphs do not deviate much from their expectation. To that end, the concentration inequality in [Warnke \(2017\)](#) will be used to bound the edge weighted degree.

It should be noted that throughout the proof, we will use c, c', c'' likewise to denote constants which may be different from line to line. Now we proceed to prove [Theorem 1](#). Let S denote the unit ball in the n -dimensional Euclidean space. Fix $\epsilon \in (0, 1)$, for example $\epsilon = \frac{1}{2}$, define an ϵ -net of the ball as follows:

$$\mathcal{N} = \{x = (x_1, \dots, x_n) \in S : \forall i, \sqrt{n}x_i/\epsilon \in \mathbb{Z}\}, \quad (\text{A.1})$$

where \mathbb{Z} denotes the set of all integers. Thus \mathcal{N} consists of all grid points of size $\epsilon\sqrt{n}$ within the unit ball. The Lemma 2.1 in [Lei and Rinaldo \(2015\)](#) shows that for any $A \in \mathbb{R}^{n \times n}$,

$$\|A\|_2 \leq (1 - \epsilon)^{-2} \sup_{x, y \in \mathcal{N}} |x^\top Ay|. \quad (\text{A.2})$$

Therefore, to bound $\|W^M - \mathbb{E}(W^M)\|_2$, we only need to bound $|x^\top(W^M - \mathbb{E}(W^M))y|$ over

all possible pairs $(x, y) \in \mathcal{N}$. For any pair of vector (x, y) , we have

$$x^\top (W^M - \mathbb{E}(W^M))y = \sum_{i,j} x_i y_j (W^M - \mathbb{E}(W^M))_{ij}. \quad (\text{A.3})$$

We split the pairs (x_i, y_j) into *light pairs*

$$\mathcal{L} = \mathcal{L}(x, y) = \{(i, j) : |x_i y_j| \leq \frac{\sqrt{D}}{n\tau_{\max}}\},$$

and into *heavy pairs*

$$\mathcal{H} = \mathcal{H}(x, y) = \{(i, j) : |x_i y_j| > \frac{\sqrt{D}}{n\tau_{\max}}\},$$

where D and τ_{\max} are defined in Theorem 1. For the light pairs, we have the following results.

Lemma 2 (*Light pairs*) *For some constant $r_1 > 0$, there exists a constant $c_1(r_1) > 0$ such that with probability at least $1 - n^{-r_1}$,*

$$\sup_{x,y \in \mathcal{N}} \left| \sum_{(i,j) \in \mathcal{L}} x_i y_j (W^M - \mathbb{E}(W^M))_{ij} \right| \leq c_1 \sqrt{D}. \quad (\text{A.4})$$

To bound the contribution of heavy pairs, we first have the following observation,

$$\sup_{x,y \in \mathcal{N}} \left| \sum_{(i,j) \in \mathcal{H}} x_i y_j (W^M - \mathbb{E}(W^M))_{ij} \right| \leq \sup_{x,y \in \mathcal{N}} \left| \sum_{(i,j) \in \mathcal{H}} x_i y_j W_{ij}^M \right| + \sup_{x,y \in \mathcal{N}} \left| \sum_{(i,j) \in \mathcal{H}} x_i y_j \mathbb{E}(W_{ij}^M) \right|. \quad (\text{A.5})$$

Recall that $\mathbb{E}(W_{ij}) \leq \alpha_n p_n$, then

$$\mathbb{E}(W_{ij}^M) = \mathbb{E} \sum_k \mathbf{1}(W_{ij} \cdot W_{ik} \cdot W_{jk} > 0) (W_{ij} + W_{ik} + W_{jk}) \leq 3n\alpha_n p_n^3. \quad (\text{A.6})$$

Then the second term in (A.5) can be bounded as follows,

$$\begin{aligned}
\left| \sum_{(i,j) \in \mathcal{H}} x_i y_j \mathbb{E}(W_{ij}^M) \right| &\leq \sum_{(i,j) \in \mathcal{H}} \frac{x_i^2 y_j^2}{|x_i y_j|} \mathbb{E}(W_{ij}^M) \\
&\leq \frac{n\tau_{\max}}{\sqrt{D}} \max_{ij} \mathbb{E}(W_{ij}^M) \sum_{(i,j)} x_i^2 y_j^2 \\
&\leq \frac{n\tau_{\max}}{\sqrt{D}} 3n\alpha_n p_n^3 \leq \frac{cD}{\sqrt{D}} \leq c\sqrt{D},
\end{aligned} \tag{A.7}$$

where the second inequality follows from the definition of heavy pairs \mathcal{H} , the third inequality follows from (A.6) and the vectors x and y are within the unit ball, and the penultimate inequality follows since

$$n\tau_{\max} \cdot 3n\alpha_n p_n^3 \leq cn^3 \alpha_n p_n^5 \leq cD, \tag{A.8}$$

by recalling $\tau_{\max} = np_n^2$. For the first term in (A.5), we have the following result.

Lemma 3 (Heavy pairs) *For some constants $r_2 > 0$, $r_3 > 0$, and any $0 < \beta < 1$, there exists a constant $c_2(r_2, r_3, \beta) > 0$ such that with probability at least $1 - n^{-r_2} - \exp(-r_3(\log n)^\beta)$,*

$$\sup_{x, y \in \mathcal{N}} \left| \sum_{(i,j) \in \mathcal{H}} x_i y_j W_{ij}^M \right| \leq c_2 \sqrt{D}. \tag{A.9}$$

Combining the results for the light and heavy pairs and recalling (A.2), we obtain

$$\|W^M - \mathbb{E}(W^M)\|_2 \leq 4 \sup_{x, y \in \mathcal{N}} \left| \sum x_i y_j (W^M - \mathbb{E}(W^M))_{ij} \right| \leq c\sqrt{D}. \tag{A.10}$$

■

Proof of Theorem 2

We make use of the framework in [Lei and Rinaldo \(2015\)](#) to bound the misclustering error rate. To fix ideas, we give some notation now. U and \tilde{U} denote the K leading eigenvectors of \mathcal{W}^M and W^M , respectively. $\hat{U} := \hat{\Theta} \hat{Y}$ corresponds to the optimal solution of the higher-

order spectral clustering algorithm in that,

$$(\hat{\Theta}, \hat{Y}) = \arg \min_{\Theta \in \mathbb{M}_{n,K}, Y \in \mathbb{R}^{K \times K}} \|\Theta Y - \tilde{U}\|_{\text{F}}^2.$$

By Lemma 1, in the WSBMs, two nodes are in the same community if and only if the corresponding rows of the population eigenvector matrix U are the same. Building on this result, in what follows, we first bound the deviation of \hat{U} from U . Then, within each true cluster, we bound the size of nodes that correspond to a large deviation of \hat{U} from U , we bound their size. After that, we show for the remaining nodes that the estimated and true communities are consistent.

First, we bound the deviation of \hat{U} from U . Davis-Kahan $\sin\Theta$ theorem (Theorem VII.3.1 of Bhatia (1997)) provides a useful technical tool for bounding the perturbation of eigenvectors from the perturbation of matrices. In particular, by Theorem 3.1 of Lei and Rinaldo (2015), there exists a $K \times K$ orthogonal matrix O such that,

$$\|\tilde{U} - UO\|_{\text{F}} \leq \frac{2\sqrt{2K}}{\lambda_K(\mathcal{W}^M)} \|W^M - \mathcal{W}^M\|_2, \quad (\text{A.11})$$

where we recall that $\lambda_K(\mathcal{W}^M)$ denotes the minimum non-zero eigenvalue of the population matrix \mathcal{W}^M . Now we proceed to bound the deviation of \hat{U} from U . Note that

$$\begin{aligned} \|\hat{U} - UO\|_{\text{F}}^2 &= \|\hat{U} - \tilde{U} + \tilde{U} - UO\|_{\text{F}}^2 \\ &\leq \|UO - \tilde{U}\|_{\text{F}}^2 + \|\tilde{U} - UO\|_{\text{F}}^2 \\ &= 2\|\tilde{U} - UO\|_{\text{F}}^2, \end{aligned} \quad (\text{A.12})$$

where the first inequality follows from our assumption that \hat{U} is the global solution of the higher-order spectral clustering algorithm and UO is a feasible solution. Then combine (A.12) with (A.11), we have

$$\|\hat{U} - UO\|_{\text{F}}^2 \leq \frac{16K}{\lambda_K^2(\mathcal{W}^M)} \|W^M - \mathcal{W}^M\|_2^2. \quad (\text{A.13})$$

Now we calculate the terms on the RHS of (A.13). Recall the definition of \mathcal{W}^M in (2.6) and the definitions of h_1 and h_2 in (2.4) and (2.5), we can easily obtain

$$\lambda_K(\mathcal{W}^M) = \frac{n}{K}(h_1 - h_2) \asymp \frac{n^2 \alpha_n p_n^3}{K}, \quad (\text{A.14})$$

and

$$\|W^M - \mathcal{W}^M\|_2 = \|W^M - \mathbb{E}(W^M) - \text{diag}(\mathcal{W}^M)\|_2 \asymp \|W^M - \mathbb{E}(W^M)\|_2. \quad (\text{A.15})$$

Combining (A.14), (A.15), and the bound in Theorem 1 with (A.13), we have

$$\|\hat{U} - UO\|_{\mathbb{F}}^2 \leq \frac{c16K^3}{n\alpha_n p_n} := \text{err}(K, n, c, \alpha_n, p_n), \quad (\text{A.16})$$

where for notational convenience, we use $\text{err}(K, n, c, \alpha_n, p_n)$ to denote $c16K^3/n\alpha_n p_n$ in what follows.

In the sequel, we proceed to bound the fraction of misclustered nodes within each true cluster. By Lemma 1, we can write $U = \Theta X$, where $\|X_{k*} - X_{l*}\|_2 = \sqrt{n_k^{-1} + n_l^{-1}}$ for all $1 \leq k < l \leq K$. Hence $UO = \Theta XO = \Theta X'$ with $X' = XO$, and $\|X'_{k*} - X'_{l*}\|_2 = \sqrt{n_k^{-1} + n_l^{-1}}$ by the orthogonality of O . Define

$$\delta_k = \min_{l \neq k} \|X'_{k*} - X'_{l*}\|_2 = \sqrt{\frac{1}{n_k} + \frac{1}{\max\{n_l : l \neq k\}}}, \quad (\text{A.17})$$

and

$$S_k = \{i \in G_k(\Theta) : \|(\hat{U}) - (UO)_{i*}\|_{\mathbb{F}} > \frac{\delta_k}{2}\}, \quad (\text{A.18})$$

where S_k is essentially the number of misclustered nodes in the true cluster k (after some permutation) as we will see soon. By the definition of S_k , it is obvious to see

$$\sum_{k=1}^K |S_k| \delta_k^2 / 4 \leq \|\hat{U} - UO\|_{\mathbb{F}}^2 = \text{err}(K, n, c, \alpha_n, p_n). \quad (\text{A.19})$$

Recall that $\delta_k = \min_{l \neq k} \|X'_{k*} - X'_{l*}\|_2 = \sqrt{\frac{1}{n_k} + \frac{1}{\max\{n_l : l \neq k\}}}$, so $n_k \delta_k^2 \geq 1$. Therefore, (A.19)

entails that

$$\sum_{k=1}^K \frac{|S_k|}{n_k} \leq 4 \cdot \|\hat{U} - UO\|_{\mathbb{F}}^2 = 4 \cdot \text{err}(K, n, c, \alpha_n, p_n). \quad (\text{A.20})$$

At last, we show that the nodes within in true community k (after some permutation) but outside S_k are correctly clustered. Before moving on, we first prove $|S_k| < n_k$. We have by (A.19) that

$$|S_k| \leq \frac{4}{\delta_k^2} \text{err}(K, n, c, \alpha_n, p_n). \quad (\text{A.21})$$

As $n_k \delta_k^2 \geq 1$, it suffices to prove

$$4 \cdot \text{err}(K, n, c, \alpha_n, p_n) < 1. \quad (\text{A.22})$$

which actually follows from the assumption (3.3) after some modification of c (c can be different from line to line). As a result, we have $|S_k| < n_k$ for every $1 \leq k \leq K$. And thus, $T_k \equiv G_k \setminus S_k \neq \emptyset$, where we recall that G_k denotes the nodes in the true community k . Let $T = \cup_{k=1}^K T_k$, we now show that the rows in $(UO)_{T^*}$ has a one to one correspondence with those in \hat{U}_{T^*} . On the one hand, for $i \in T_k$ and $j \in T_l$ with $l \neq k$, $\hat{U}_{i^*} \neq \hat{U}_{j^*}$, otherwise one can have the following contradiction

$$\begin{aligned} \max\{\delta_k, \delta_l\} &\leq \|(UO)_{i^*} - (UO)_{j^*}\|_2 \\ &\leq \|(UO)_{i^*} - \hat{U}_{i^*}\|_2 + \|(UO)_{j^*} - \hat{U}_{j^*}\|_2 \\ &< \frac{\delta_k}{2} + \frac{\delta_l}{2}, \end{aligned} \quad (\text{A.23})$$

where the first and last inequality follows from (A.17) and (A.18), respectively. On the other hand, for $i, j \in T_k$, we have $\hat{U}_{i^*} = \hat{U}_{j^*}$, because otherwise U_{T^*} has more than K distinct rows contradicting the fact that the output community size is K .

As a result, we have proved the membership is correctly recovered outside of $\cup_{k=1}^K S_k$ and the rate of misclustered nodes in S_k is bounded as in (A.20), and therefore the conclusion of Theorem 2 is arrived. ■

B. Proof of auxiliary Lemmas

Proof of Lemma 2

We will make use of the typical bounded differences inequality established in [Warnke \(2016\)](#) to control the contribution of the light pairs. To fix ideas, we reproduce the result that we will use in the following proposition.

Proposition 1 (Theorem 1.2 of [Warnke \(2016\)](#)) *Let $X = (X_1, \dots, X_N)$ be a family of independent random variables with X_k taking values in a set Λ_k . Let $\Gamma \subseteq \prod_{j \in [N]} \Lambda_j$ be an event and assume that function $f : \prod_{j \in [N]} \Lambda_j \rightarrow \mathbb{R}$ satisfies the following typical Lipschitz condition.*

(TL) *There are numbers $(c_k)_{k \in [N]}$ and $(d_k)_{k \in [N]}$ with $c_k \leq d_k$ such that, whenever $x, \tilde{x} \in \prod_{j \in [N]} \Lambda_j$ differ only in the k th coordinate, we have*

$$|f(x) - f(\tilde{x})| \leq \begin{cases} c_k, & \text{if } \Gamma \text{ holds,} \\ d_k, & \text{otherwise.} \end{cases} \quad (\text{B.1})$$

Then for all numbers $(\gamma_k)_{k \in [N]}$ with $\gamma_k \in (0, 1]$ there is an event $\mathcal{B} = \mathcal{B}(\Gamma, (\gamma_k)_{k \in [N]})$ satisfying

$$\mathbb{P}(\mathcal{B}) \leq \mathbb{P}(X \notin \Gamma) \sum_{k \in [N]} \gamma_k^{-1} \quad \text{and} \quad \neg \mathcal{B} \subseteq \Gamma, \quad (\text{B.2})$$

such that for all $t \geq 0$ we have

$$\mathbb{P}(f(X) \geq \mathbb{E}f(X) + t \text{ and } \neg \mathcal{B}) \leq \exp\left(-\frac{t^2}{2 \sum_{k \in [N]} (c_k + e_k)^2}\right), \quad (\text{B.3})$$

where $e_k = \gamma_k(d_k - c_k)$. In many applications, the following simple consequence of (B.2) and (B.3) suffices:

$$\mathbb{P}(f(X) \geq \mathbb{E}f(X) + t) \leq \exp\left(-\frac{t^2}{2 \sum_{k \in [N]} (c_k + \gamma_k(d_k - c_k))^2}\right) + \mathbb{P}(X \notin \Gamma) \sum_{k \in [N]} \gamma_k^{-1}. \quad (\text{B.4})$$

Now we proceed to bound the light pairs. Define

$$u_{ij} = x_i y_j \mathbf{1}((i, j) \in \mathcal{L}) + x_j y_i \mathbf{1}((j, i) \in \mathcal{L})$$

for all $i, j = 1, \dots, n$. Then

$$\begin{aligned} \sum_{(i,j) \in \mathcal{L}} x_i y_j (W^M - \mathbb{E}(W^M))_{ij} &= \sum_{i < j} \sum_{k \neq i, j} \mathbf{1}(W_{ij} W_{ik} W_{jk} > 0) (W_{ij} + W_{ik} + W_{jk}) u_{ij} \\ &\quad - \sum_{i < j} \sum_{k \neq i, j} \mathbb{E}(\mathbf{1}(W_{ij} W_{ik} W_{jk} > 0) (W_{ij} + W_{ik} + W_{jk})) u_{ij}. \end{aligned} \quad (\text{B.5})$$

To use the result in Proposition 1, we define

$$f(W) = \sum_{i < j} \sum_{k \neq i, j} \mathbf{1}(W_{ij} W_{ik} W_{jk} > 0) (W_{ij} + W_{ik} + W_{jk}) u_{ij}. \quad (\text{B.6})$$

It is obvious that f is a function of independent variables W_{ij} ($i, j = 1, \dots, n$). Now we proceed to bound the effect on f when only one element of W_{ij} is changed, namely, we specify (B.1) in our setting. Suppose W_{ij} changes, then the effect on f may be “large” on the term involving u_{ij} . In particular, the effect can be bounded as

$$\sum_{k \neq i, j} \mathbf{1}(W_{ik} \cdot W_{jk} > 0) (1 + W_{ik} + W_{jk}) u_{ij}. \quad (\text{B.7})$$

On the other hand, the effect on f may be “small” on the term involving u_{ik} or u_{jk} . In particular, the effect can be bounded as $3u_{ik}$ or $3u_{jk}$, respectively, provided that k is the common neighborhood of i and j . To further bound the “large” effect and “small” effect, we define

$$\tau_{ij} = \sum_{k \neq i, j} \mathbf{1}(W_{ik} \cdot W_{jk} > 0) (1 + W_{ik} + W_{jk}), \quad (\text{B.8})$$

by recalling the formula in (B.7) and define the “good set” Γ

$$\Gamma = \{(W_{ij}) : \max_{ij} \tau_{ij} \leq c\tau_{\max}\}, \quad (\text{B.9})$$

where c is large enough. We want to prove that the probability of W outside the good set vanishes when n goes to infinity. To this end, we first bound the expectation of

$$\delta_{ij}^k := \mathbf{1}(W_{ik} \cdot W_{jk} > 0)(1 + W_{ik} + W_{jk}).$$

We have

$$\mathbb{E}(\delta_{ij}^k) = \mathbb{E}(\mathbf{1}(W_{ik} \cdot W_{jk} > 0)(1 + W_{ik} + W_{jk})) \leq c' p_n^2. \quad (\text{B.10})$$

Now we use the Bernstein's inequality to bound the the probability of W outside the good set Γ .

$$\begin{aligned} \mathbb{P}(W \notin \Gamma) &\leq n^2 \mathbb{P}(\tau_{ij} > c\tau_{\max}) \\ &\leq n^2 \mathbb{P}\left(\sum_{k \neq i, j} \mathbf{1}(W_{ik} \cdot W_{jk} > 0)(1 + W_{ik} + W_{jk}) > c\tau_{\max}\right) \\ &\leq n^2 \mathbb{P}\left(\sum_{k \neq i, j} [\mathbf{1}(W_{ik} \cdot W_{jk} > 0)(1 + W_{ik} + W_{jk}) - \mathbb{E}(\delta_{ij}^k)] > c\tau_{\max} - c' n p_{\max}\right) \\ &\leq n^2 \mathbb{P}\left(\sum_{k \neq i, j} [\mathbf{1}(W_{ik} \cdot W_{jk} > 0)(1 + W_{ik} + W_{jk}) - \mathbb{E}(\delta_{ij}^k)] > c'' \tau_{\max}\right) \\ &\leq n^2 \exp\left(-\frac{c\tau_{\max}^2}{c' n p_n^2 + c'' \tau_{\max}}\right) \leq n^2 \exp(-c''' \tau_{\max}) \\ &\leq n^2 \exp(-\log n^c) \leq n^{-c+2} \leq n^{-c'}, \end{aligned} \quad (\text{B.11})$$

where we used the following facts, $\tau_{\max} \geq c \log n$ which is implied by $\tau_{\max} = n p_n^2$ and $p_n^2 \geq c \log n / n$, $\mathbb{E}((\delta_{ij}^k)^2) \leq c \mathbb{E}(\delta_{ij}^k)$ and (B.10).

Next, we continue to bound the effect of changing one element W_{ij} of W on $f(W)$. Before that, we first have the following observation. Recalling (B.8), under the good event Γ , we have

$$\sum_{k \neq i, j} \mathbf{1}(W_{ik} \cdot W_{jk} > 0) \leq \tau_{ij} = \sum_{k \neq i, j} \mathbf{1}(W_{ik} \cdot W_{jk} > 0)(1 + W_{ik} + W_{jk}) \leq c\tau_{\max}, \quad (\text{B.12})$$

which means that the number of k being the common neighborhood of i and j is not larger

than $c\tau_{\max}$ under the good event Γ . Recall that, the “large” effect can be bounded as

$$\sum_{k \neq i, j} \mathbf{1}(W_{ik} \cdot W_{jk} > 0)(1 + W_{ik} + W_{jk})u_{ij},$$

and the “small” effect can be bounded as $3u_{ik}$ or $3u_{jk}$, respectively, provided that k is the common neighborhood of i and j . Therefore, combining the “large” and “small” effects, under the good event Γ , the total effect of changing one element W_{ij} in $f(W)$ can be upper bounded as

$$c_{ij} \leq c\tau_{\max}u_{ij} + 3 \sum_{k: W_{ik}W_{jk} > 0} u_{ik} \leq c\tau_{\max}u_{ij} + c'\tau_{\max}u_{ik}. \quad (\text{B.13})$$

On the other hand, when the bad event $\neg\Gamma$ occurs, the total effect of changing one element W_{ij} in $f(W)$ becomes

$$d_{ij} \leq 3nu_{ij} + 3nu_{ik}. \quad (\text{B.14})$$

We are now moving towards (B.3) in our setting. Define $\gamma_{ij} = \frac{1}{n}$ for all i, j . Then $e_{ij} = \gamma_{ij}(d_{ij} - c_{ij}) = o(c_{ij})$ by recalling the definition of τ_{\max} . And we have

$$\sum_{ij} c_{ij}^2 \leq c\tau_{\max}^2 \sum_{ij} u_{ij}^2, \quad (\text{B.15})$$

and

$$\mathbb{P}(\mathcal{B}) \leq \mathbb{P}(W \notin \Gamma) \sum_{i, j} \gamma_{ij}^{-1} = n^3 \mathbb{P}(W \notin \Gamma) \leq \exp(- (c' - 3) \log n). \quad (\text{B.16})$$

Therefore, combining (B.15) with (B.3), we have for large enough c that

$$\begin{aligned} \mathbb{P}(f(W) - \mathbb{E}f(W) > c\sqrt{D} \cap \neg\mathcal{B}) &\leq \exp\left(-\frac{c^2 D}{c'\tau_{\max}^2 \sum_{ij} u_{ij}^2}\right) \\ &\leq \exp\left(-\frac{c^2 \tau_{\max}^2 n \alpha_n p_n}{c'\tau_{\max}^2 \sum_{ij} u_{ij}^2}\right) \\ &\leq \exp(-cn\sqrt{n\alpha_n p_n}) \leq \exp(-c''n), \end{aligned} \quad (\text{B.17})$$

where the second inequality follows from the fact that

$$\sum_{ij} u_{ij}^2 \leq c \max_{ij} |u_{ij}| \sum_{ij} |x_i y_j| \leq c \frac{\sqrt{D}}{n\tau_{\max}} \|x\|_2 \|y\|_2 \leq c' \frac{\sqrt{D}}{n\tau_{\max}},$$

and the last inequality is implied by $\alpha_n p_n > c''(\log n)^\beta/n$ for some small constant c'' . Finally, it is obvious that the event $\{W \notin \Gamma\}$ does not depend on the choice of vectors x and y , thus taking the supremum over all x and y , and combining (B.16) and (B.17) with (B.4), we obtain

$$\mathbb{P}(\sup_{x,y \in \mathcal{N}} \left| \sum_{(i,j) \in \mathcal{L}} x_i y_j (W^M - \mathbb{E}(W^M))_{ij} \right| \geq c_1 \sqrt{D}) \leq \exp(-(c'' - \log 5)n) + \exp(-(c' - 3)\log n), \quad (\text{B.18})$$

where we used the fact that $|\mathcal{N}| \leq \exp(n \log 5)$. Since c'' and c' are large enough, the probability in (B.18) decays polynomially with n . \blacksquare

Proof of Lemma 3

The proof follows a similar strategy as in Feige and Ofek (2005); Paul et al. (2018); Lei and Rinaldo (2015), among others. We will focus on the heavy pairs (i, j) such that $x_i > 0, y_j > 0$ and the set

$$\mathcal{H}_1 = \{(i, j) \in \mathcal{H} : x_i > 0, y_j > 0\}.$$

The other three cases can be treated similarly. We will need the following notation:

- $I_1 = \{i : \frac{1}{2n^{1/2}} \leq x_i \leq \frac{1}{n^{1/2}}\}$, $I_s = \{i : \frac{2^{s-1}}{2n^{1/2}} \leq x_i \leq \frac{2^s}{2n^{1/2}}\}$ for $s = 2, 3, \dots, \lceil \log_2 2n^{1/2} \rceil$.
 $J_1 = \{j : \frac{1}{2n^{1/2}} \leq y_j \leq \frac{1}{n^{1/2}}\}$, $J_t = \{j : \frac{2^{t-1}}{2n^{1/2}} \leq y_j \leq \frac{2^t}{2n^{1/2}}\}$ for $t = 2, 3, \dots, \lceil \log_2 2n^{1/2} \rceil$.
- $e(I, J)$ denotes the weights of distinct edges in the motif-based network W^M between nodes sets I and J . $e(I, J) = \sum_{i \in I} \sum_{j \in J} W_{ij}^M$, if $I \cap J = \emptyset$; $\sum_{(i,j) \in I \times J \setminus (I \cap J)^2} W_{ij}^M + \sum_{(i,j) \in (I \cap J)^2, i < j} W_{ij}^M$, if $I \cap J \neq \emptyset$.
- $\mu(I, J) = \mathbb{E}(e(I, J))$, and $\bar{\mu} = |I||J| \frac{\Delta}{n}$, where we define $\Delta = n^2 \alpha_n p_n^3$.

- $\lambda_{st} = e(I_s, J_t)/\bar{\mu}_{st}$, where $\bar{\mu}_{st} = \bar{\mu}(I_s, J_t)$.
- $\alpha_s = |I_s|2^{2s}/n$, $\beta_t = |J_t|2^{2t}/n$, and $\sigma_{st} = \lambda_{st} \frac{\sqrt{D}}{\tau_{\max}} 2^{-(s+t)}$.

We begin by providing the following two results which play a key role in the proof.

Lemma 4 (Bounded degree) *Let*

$$d_i^M = \sum_j \sum_{k \neq i, j} (\mathbf{1}(W_{ij} \cdot W_{ik} \cdot W_{jk} > 0)(W_{ij} + W_{ik} + W_{jk}))$$

denote the weighted triangle degree of node i . If $\alpha_n p_n^2 > c''(\log n)^\beta/n$ for any $0 < \beta < 1$, then for all i and some constant $r_4, r_5 > 0$, there exists a constant $c_3(r_4, r_5) > 0$ such that

$$d_i^M \leq c_3 \Delta,$$

with probability larger than $1 - n^{-r_4} - \exp(-r_5(\log n)^\beta)$.

Lemma 5 (Bounded discrepancy) *For a constant $r_6 > 0$, there exists constants $c_4 = c_4(r_6) > 0$, $c_5 = c_5(r_6) > 0$ such that with probability larger than $1 - 2n^{-r_6}$, for any $I, J \subseteq [n]$ with $[I] \leq [J]$, at least one of the following statements holds:*

- $\frac{e(I, J)}{\bar{\mu}(I, J)} \leq ec_4$,
- $e(I, J) \log \frac{e(I, J)}{\bar{\mu}(I, J)} \leq c_5 \tau_{\max} |J| \log \frac{n}{|J|}$.

Define \mathcal{E} be the event that the results of Lemma 4 and 5 hold. In the sequel, we proceed to bound the heavy pairs under the event \mathcal{E} . We first have the following facts.

$$\begin{aligned}
& \sum_{(i,j) \in \mathcal{H}_1} x_i y_j W_{ij}^M \\
& \leq 2 \sum_{2^{(s+t)} \geq \frac{\sqrt{D}}{\tau_{\max}}} e(I_s, J_t) \frac{2^s}{2n^{1/2}} \frac{2^t}{2n^{1/2}} \\
& \leq 2 \frac{1}{4} \sum_{2^{(s+t)} \geq \frac{\sqrt{D}}{\tau_{\max}}} \frac{e(I_s, J_t)}{|I_s||J_t|n\alpha_n p_{\max}^3} \frac{D}{\tau_{\max}} \frac{2^s |I_s| 2^t |J_t|}{n^2} \\
& = \frac{1}{2} \sqrt{D} \sum_{2^{(s+t)} \geq \frac{\sqrt{D}}{\tau_{\max}}} \frac{e(I_s, J_t)}{\bar{\mu}(I_s, J_t)} \frac{\sqrt{D}}{\tau_{\max}} 2^{-(s+t)} \frac{2^{2s} |I_s| 2^{2t} |J_t|}{n^2} \\
& = \frac{1}{2} \sqrt{D} \sum_{2^{(s+t)} \geq \frac{\sqrt{D}}{\tau_{\max}}} \alpha_s \beta_t \sigma_{st}.
\end{aligned}$$

We will prove that $\sum_{2^{(s+t)} \geq \frac{\sqrt{D}}{\tau_{\max}}} \alpha_s \beta_t \sigma_{st}$ is bounded by some constant. To that end, following Feige and Ofek (2005); Lei and Rinaldo (2015); Paul et al. (2018), we split the set of pairs $\mathcal{C} : \{(s, t) : 2^{(s+t)} \geq \frac{\sqrt{D}}{\tau_{\max}}, |I_s| \leq |J_t|\}$ into six sets and we will show that the contribution of each part is bounded. We will use the following facts repeatedly,

$$\sum_s \alpha_s \leq 4(1/2)^{-2} = 16, \quad \sum_t \beta_t \leq 4(1/2)^{-2} = 16.$$

- $\mathcal{C}_1 : \{(s, t) \in \mathcal{C}, \sigma_{st} \leq 1\}$.

$$\sum_{s,t} \alpha_s \beta_t \sigma_{st} \mathbf{1}\{(s, t) \in \mathcal{C}_1\} \leq \sum_{s,t} \alpha_s \beta_t \leq 256.$$

- $\mathcal{C}_2 : \{(s, t) \in \mathcal{C} \setminus \mathcal{C}_1, \lambda_{st} \leq ce\}$.

Note that

$$\sigma_{st} = \lambda_{st} \frac{\sqrt{D}}{\tau_{\max}} 2^{-(s+t)} \leq \lambda_{st} \leq ce,$$

so we have

$$\sum_{s,t} \alpha_s \beta_t \sigma_{st} \mathbf{1}\{(s, t) \in \mathcal{C}_2\} \leq ce.$$

- $\mathcal{C}_3 : \{(s, t) \in \mathcal{C} \setminus (\mathcal{C}_1 \cup \mathcal{C}_2), 2^{s-t} \geq \frac{\sqrt{D}}{\tau_{\max}}\}$.

Note that by Lemma 4,

$$\lambda_{st} = \frac{e(I_s, J_t)}{\bar{\mu}_{st}} \leq c \frac{|I_s| \Delta}{|I_s| |J_t| \Delta / n} \leq c \frac{n}{|J_t|}.$$

Hence

$$\sigma_{st} = \lambda_{st} \frac{\sqrt{D}}{\tau_{\max}} 2^{-(s+t)} \leq c \frac{n}{|J_t|} \frac{\sqrt{D}}{\tau_{\max}} 2^{-(s+t)}.$$

And consequently

$$\sum_t \beta_t \sigma_{st} \leq c \sum_t 2^{2t} \frac{|J_t|}{n} \cdot \frac{n}{|J_t|} \frac{\sqrt{D}}{\tau_{\max}} 2^{-(s+t)} = c \sum_t \frac{\sqrt{D}}{\tau_{\max} 2^{s-t}} \leq c,$$

where the last inequality follows from the fact that the non-zero summands over t are bounded by 1 for a geometric sequence. Finally, we have

$$\sum_{s,t} \alpha_s \beta_t \sigma_{st} \mathbf{1}\{(s, t) \in \mathcal{C}_3\} \leq c \sum_s \alpha_s \leq c'.$$

- $\mathcal{C}_4 : \{(s, t) \in \mathcal{C} \setminus (\mathcal{C}_1 \cup \mathcal{C}_2 \cup \mathcal{C}_3), \log \lambda_{st} > \frac{1}{4}[2t \log 2 + \log(1/\beta_t)]\}$.

By Lemma 5, we have

$$\lambda_{st} \log \lambda_{st} |I_s| |J_t| \frac{\Delta}{n} = \frac{e(I_s, J_t)}{\bar{\mu}(I_s, J_t)} \log \frac{e(I_s, J_t)}{\bar{\mu}(I_s, J_t)} \bar{\mu}(I_s, J_t) \leq c_5 \tau_{\max} |J_t| \log \frac{n}{|J_t|}.$$

Note that $\frac{\tau_{\max}}{\Delta} = \frac{\tau_{\max}^2}{D}$ by the definition of D, Δ and $p_n \geq \frac{\log n}{n}$. Then we have

$$\begin{aligned} \sigma_{st} \alpha_s &\leq \lambda_{st} \frac{\sqrt{D}}{\tau_{\max}} 2^{-(s+t)} \frac{|I_s| 2^{2s}}{n} \\ &\leq c_5 \frac{1}{\log \lambda_{st}} \frac{\tau_{\max}^2}{D} \log \left(\frac{n}{|J_t|} \right) \frac{\sqrt{D}}{\tau_{\max}} 2^{s-t} \\ &\leq c_5 \frac{1}{\log \lambda_{st}} \frac{2^{s-t}}{\sqrt{D}/\tau_{\max}} \left[2t \log 2 + \log \left(\frac{1}{\beta_t} \right) \right] \\ &\leq 4c_5 \frac{2^{s-t}}{\sqrt{D}/\tau_{\max}}. \end{aligned} \tag{B.19}$$

And then

$$\begin{aligned} \sum_{s,t} \alpha_s \beta_t \sigma_{st} \mathbf{1}\{(s,t) \in \mathcal{C}_4\} &= \sum_t \beta_t \sum_s \sigma_{st} \alpha_s \mathbf{1}\{(s,t) \in \mathcal{C}_4\} \\ &\leq 4c_5 \sum_t \beta_t \sum_s \frac{2^{s-t}}{\sqrt{D}/\tau_{\max}} \mathbf{1}\{(s,t) \in \mathcal{C}_4\} \leq 4c_5 \sum_t \beta_t \leq c', \end{aligned}$$

where we used the fact that $(s,t) \notin \mathcal{C}_3$.

- $\mathcal{C}_5 : \{(s,t) \in \mathcal{C} \setminus (\mathcal{C}_1 \cup \mathcal{C}_2 \cup \mathcal{C}_3 \cup \mathcal{C}_4), 2t \log 2 \geq \log(1/\beta_t)\}$.

Since $(s,t) \notin \mathcal{C}_4$, we have

$$\log \lambda_{st} \leq \frac{1}{4} [2t \log 2 + \log \beta_t^{-1}] \leq ct \log 2,$$

and thus $\lambda_{st} \leq c2^t$. Because $(s,t) \notin \mathcal{C}_1$, we have

$$1 \leq \sigma_{st} = \lambda_{st} \frac{\sqrt{D}}{\tau_{\max}} 2^{-(s+t)} \leq c \frac{\sqrt{D}}{\tau_{\max}} 2^{-s}.$$

And because $(s,t) \notin \mathcal{C}_2$, we have $\log \lambda_{st} \geq c'$. Thus by (B.19) and the definition of \mathcal{C}_5 , we have

$$\sigma_{st} \alpha_s \leq c \frac{2^{s-t}}{\sqrt{D}/\tau_{\max}} \cdot 4t \log 2.$$

Consequently,

$$\begin{aligned} \sum_{s,t} \alpha_s \beta_t \sigma_{st} \mathbf{1}\{(s,t) \in \mathcal{C}_5\} &= \sum_t \beta_t \sum_s \sigma_{st} \alpha_s \mathbf{1}\{(s,t) \in \mathcal{C}_5\} \\ &\leq c \sum_t \beta_t \sum_s \frac{2^{s-t}}{\sqrt{D}/\tau_{\max}} 4t \\ &\leq c \sum_t \beta_t t 2^{-t} \sum_s \frac{2^s}{\sqrt{D}/\tau_{\max}} \\ &\leq c \sum_t \beta_t \leq c', \end{aligned}$$

where the last inequality follows from the fact that the non-zero summands over s are bounded by 1 for a geometric sequence.

- $\mathcal{C}_6 : \{(s, t) \in \mathcal{C} \setminus (\mathcal{C}_1 \cup \mathcal{C}_2 \cup \mathcal{C}_3 \cup \mathcal{C}_4 \cup \mathcal{C}_5)\}$.

Since $(s, t) \notin \mathcal{C}_4 \cup \mathcal{C}_2 \cup \mathcal{C}_5$, we have

$$0 < \log \lambda_{st} \leq \frac{1}{4}[2t \log 2 + \log \beta_t^{-1}] \leq \frac{1}{2} \log \beta_t^{-1} \leq \log \beta_t^{-1}.$$

Then

$$\begin{aligned} \sum_{s,t} \alpha_s \beta_t \sigma_{st} \mathbf{1}\{(s, t) \in \mathcal{C}_6\} &= \sum_s \alpha_s \sum_t \beta_t \lambda_{st} \frac{\sqrt{D}}{\tau_{\max}} 2^{-(s+t)} \mathbf{1}\{(s, t) \notin \mathcal{C}_6\} \\ &\leq \sum_s \alpha_s \sum_t \frac{\sqrt{D}}{\tau_{\max}} 2^{-(s+t)} \mathbf{1}\{(s, t) \notin \mathcal{C}_6\} \\ &\leq c \sum_s \alpha_s \leq c'. \end{aligned}$$

Putting these pieces together, and combining (A.6), for any fixed $x, y \in \mathcal{H}$, we have

$$\sum_{(i,j) \in \mathcal{H}} x_i y_j W_{ij}^M \leq c\sqrt{D},$$

under the event \mathcal{E} . Taking the supremum and combining the results of Lemma 4 and 5, we arrive the conclusion of Lemma 3. \blacksquare

Proof of Lemma 4

We will make use of Warnke (2017) to bound the degree. For reference, we reproduce the result as the following proposition.

Proposition 2 (Theorem 9 of Warnke (2017)) *Let $(Y_i), i \in \mathcal{I}$ be a collection of non-negative random variables with $\sum_{i \in \mathcal{I}} \mathbb{E}(Y_i) \leq \mu$. Assume that \sim is a symmetric relation on \mathcal{I} such that each Y_i with $i \in \mathcal{I}$ is independent of $\{Y_j : j \in \mathcal{I}, j \not\sim i\}$. Let $Z_C = \max \sum_{i \in \mathcal{J}} Y_i$, where the maximum is taken over all sets $\mathcal{J} \subset \mathcal{I}$ such that $\max_{j \in \mathcal{J}} \sum_{i \in \mathcal{J}, i \sim j} Y_i \leq C$. Then for all $C, t > 0$, we have*

$$\mathbb{P}(Z_C \geq \mu + t) \leq \min \left\{ \exp \left(- \frac{t^2}{2C(\mu + t/3)} \right), \left(1 + \frac{t}{2\mu} \right)^{-t/2C} \right\}.$$

Now we proceed to bound the degree. First, we have the observation that

$$\begin{aligned} \mathbb{E}d_i^M &= \mathbb{E}\left[\sum_j \sum_{k \neq i, j} (\mathbf{1}(W_{ij}W_{ik}W_{jk} > 0)(W_{ij} + W_{ik} + W_{jk}))\right] \\ &\leq 3n^2\alpha_n p_{\max}^3 \leq c\Delta, \end{aligned}$$

where we recall that $\Delta = n^2\alpha_n p_n^3$. Then let I_i be the set of all triangles that includes node i and denote

$$M_\theta := \mathbf{1}(W_{ij} \cdot W_{ik} \cdot W_{jk} > 0)(W_{ij} + W_{ik} + W_{jk})$$

with the index $\theta = \{i, j, k\} \in I_i$. Recall the good event Γ we defined in (B.9), then under the good event, every pair of nodes has at most $C = c\tau_{\max}$ common neighbors, and the good event holds with probability larger than $1 - n^{-c''}$. It is clear that two triangles belonging to the set I_i are independent if they do not share any edges. Let \sim denote a relation such that $\theta_1 \sim \theta_2$ holds if θ_1 and θ_2 share an edge. For any M_{ijk} , the good event restricts the number of triangles in the set I_i that are dependent with M_{ijk} to $2C$.

Define $J_i \subseteq I_i$ as

$$J_i = \{\theta : \max_{\theta_1 \in J_i} |\theta_2 \in J; \theta_1 \text{ and } \theta_2 \text{ share at least one edge}| \leq 2C\}.$$

Then, we immediately have

$$\max_{\theta_2 \in J_i} \sum_{\theta_1 \in J_i: \theta_1 \sim \theta_2} M_\theta \leq 3 \cdot 2C \leq c\tau_{\max}, \quad \sum_{\theta \in J_i} \mathbb{E}(M_\theta) \leq \Delta.$$

Take $t = \mu = \Delta$, then the results in Proposition 2 imply,

$$\begin{aligned} &\mathbb{P}(\max_{J_i} \sum_{\theta \in J_i} M_\theta \geq 2\Delta) \\ &\leq \min\left\{\exp\left(-\frac{\Delta^2}{6C(\Delta + \Delta/3)}\right), \left(1 + \frac{\Delta}{2\Delta}\right)^{-\Delta/6C}\right\} \\ &= \min\left\{\exp\left(-\frac{\Delta}{c\tau_{\max}}\right), \left(\frac{3}{2}\right)^{-\Delta/c\tau_{\max}}\right\} \\ &\leq \exp(-c'(\log n)^\beta), \end{aligned}$$

where the last inequality follows from the assumption that $\frac{\Delta}{\tau_{\max}} \geq cn\alpha_n p_n \geq c'(\log n)^\beta$ with $0 < \beta < 1$. Under the good event, we have $J_i^* = I_i$, and thus $\max_{J_i} \sum_{\theta \in J_i} M_\theta = d_i^M$. Consequently,

$$\begin{aligned} \mathbb{P}(d_i^M \geq 2\Delta) &\leq \exp(-c'(\log n)^\beta) + P(W \notin \Gamma) \\ &\leq n^{-c''} + \exp(-c'(\log n)^\beta). \end{aligned}$$

■

Proof of Lemma 5

Recall that $\bar{\mu} = |I||J|\frac{\Delta}{n}$ with $\Delta = n^2\alpha_n p_n^3$. So if $|J| > \frac{n}{e}$, then

$$\frac{e(I, J)}{\bar{\mu}(I, J)} = \frac{\sum_{i \in I} \max_i d_i^M}{|I|\Delta/e} \leq \frac{c|I|\Delta}{|I|\Delta/e} \leq c'e,$$

which is the case (a) in the lemma.

Now we prove the case (b) also holds. Denote S as the set of all 3-tuples such that each tuple has one vertex in each of the sets I and J . Then

$$e(I, J) = \sum_{\theta \in S(I, J)} W_\theta^M,$$

and

$$\mathbb{E}\left(\sum_{\theta \in S(I, J)} W_\theta^M\right) \leq |I||J|\Delta/n = \bar{\mu}(I, J).$$

Since $e(I, J)$ is the sum of dependent variables, next we use the concentration inequality in Proposition 2 to bound $e(I, J)$. Recall the good event Γ we defined in (A.19), under the good event, every pair of nodes has at most $C = c\tau_{\max}$ common neighbors, and the good event holds with probability larger than $1 - n^{-c''}$. Define $S^* \subset S$ be the set such that any W_θ^M depends on $2C$ other W_θ^M . Then under the good event, we have

$$\max_{\theta_1 \in S^*} \sum_{\theta_2 \in S^*(I, J), \theta_2 \sim \theta_1} W_\theta^M \leq c\tau_{\max}.$$

Let $t = (l - 1)\bar{\mu}(I, J)$, and apply Proposition 2, we can obtain

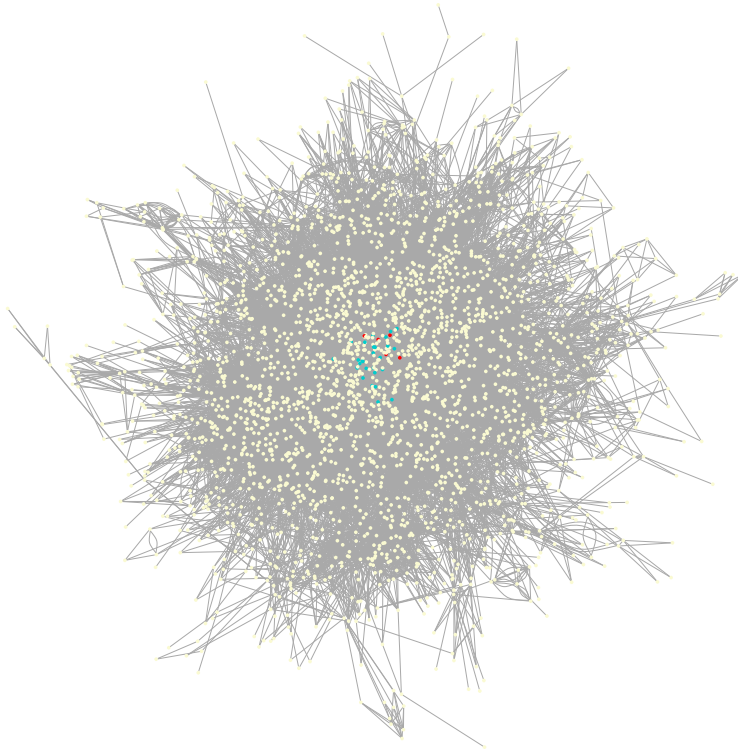
$$\begin{aligned}
\mathbb{P}(e(I, J) \geq l\bar{\mu}(I, J)) &\leq \exp\left(-\frac{t}{4\tau_{\max}}\log\left(1 + \frac{t}{2\bar{\mu}(I, J)}\right)\right) \\
&\leq \exp\left(-\frac{(\bar{\mu}(I, J) + t)\log\left(1 + \frac{t}{\bar{\mu}(I, J)}\right) - t}{\tau_{\max}}\right) \\
&= \exp\left(\frac{l \log l\bar{\mu}(I, J) - (l - 1)\bar{\mu}(I, J)}{\tau_{\max}}\right), \\
&\leq \exp\left(-\frac{1}{2}\frac{l \log l\bar{\mu}(I, J)}{\tau_{\max}}\right),
\end{aligned}$$

where the second inequality follows from the fact that

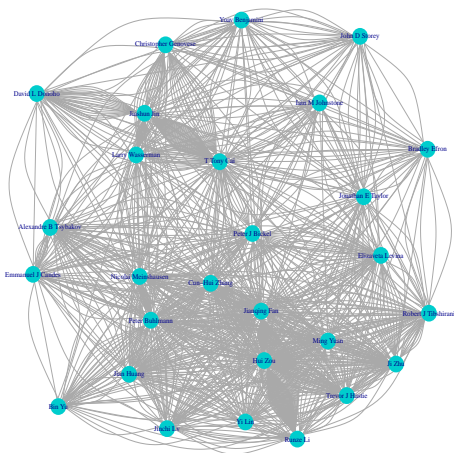
$$\bar{\mu}(I, J)\log l - (l - 1)\bar{\mu}(I, J) \leq (l - 1)\bar{\mu}(I, J)/2\log(1 + (l - 1)/2),$$

for large enough l , and the last inequality holds when $l \geq 8$. The remaining part of the proof is almost the same as that in Paul et al. (2018); Feige and Ofek (2005); Lei and Rinaldo (2015), hence we omit it. ■

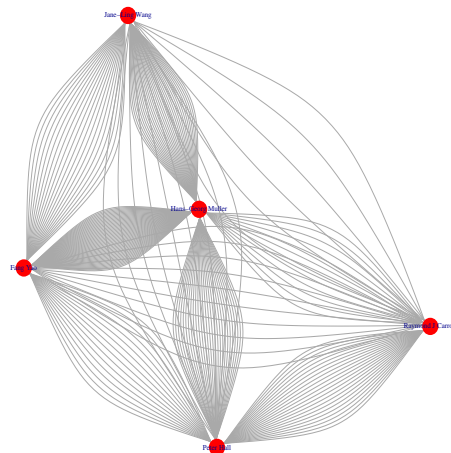
C. Clustering results in real data analysis



(a) Detected communities

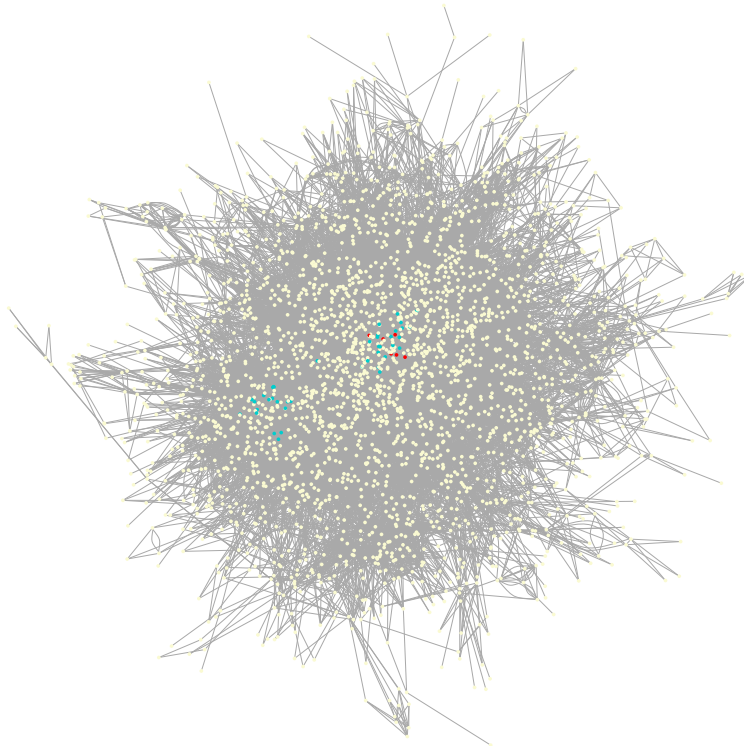


(b) High-dimensional statistics community

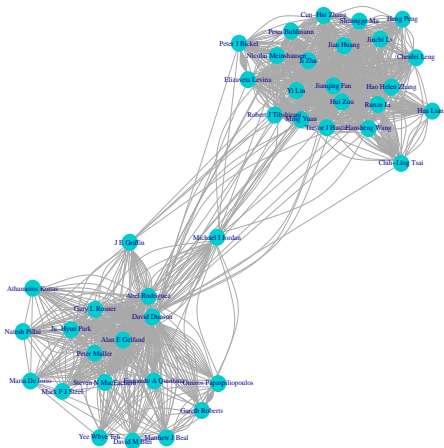


(c) Non-parametric statistics and Functional analysis community

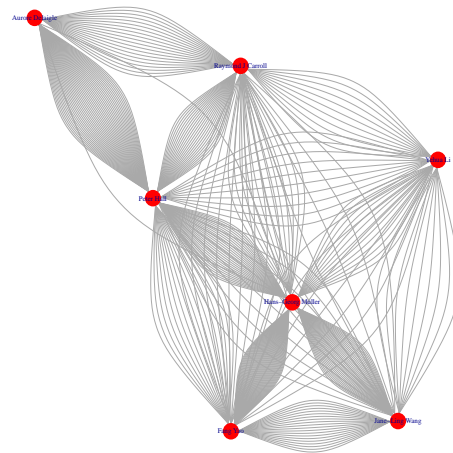
Figure 10: The clustering results for the statisticians' citation network by the motif-based spectral clustering. (a) is the general clustering results, and (b) and (c) are specific communities.



(a) Detected communities

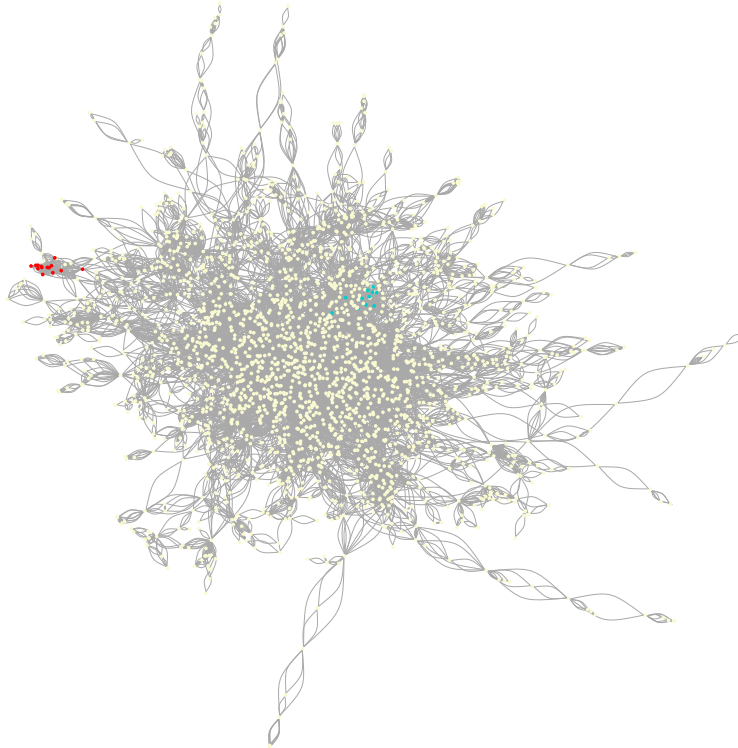


(b) High-dimensional and Bayesian statistics *mixed* community

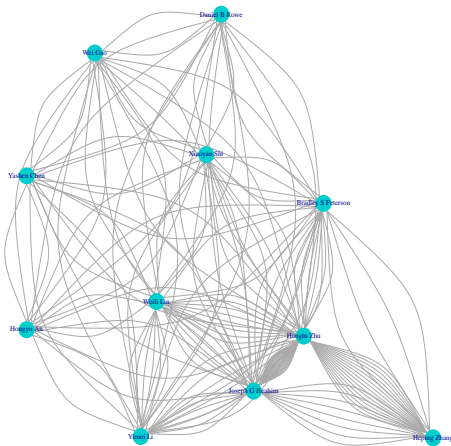


(c) Non-parametric statistics and Functional analysis community

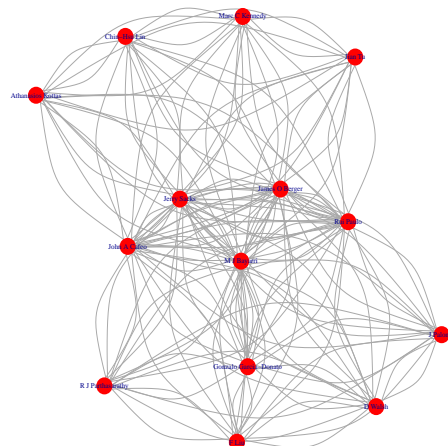
Figure 11: The clustering results for the statisticians' citation network by the edge-based spectral clustering. (a) is the general clustering results, and (b) and (c) are specific communities.



(a) Detected communities

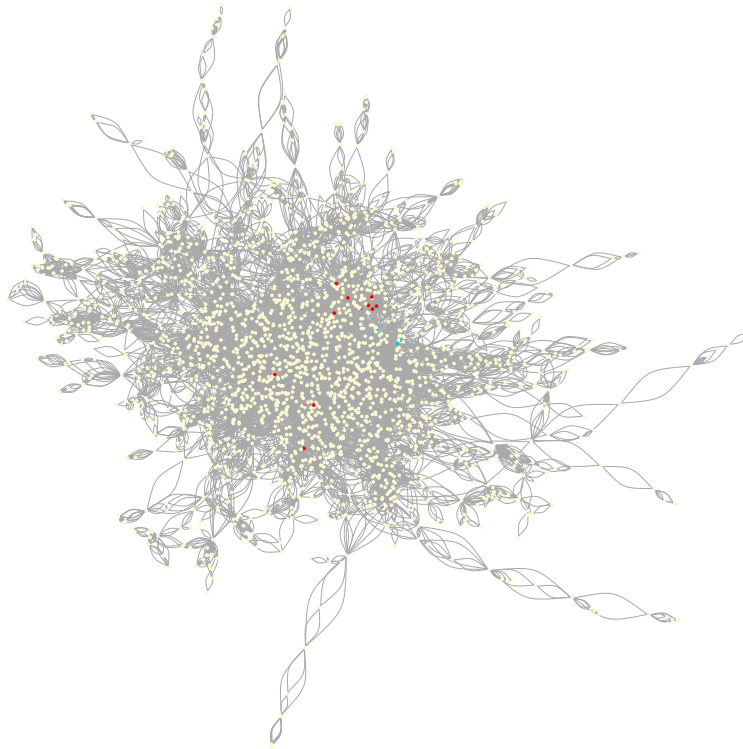


(b) Biostatistics and medical statistics community

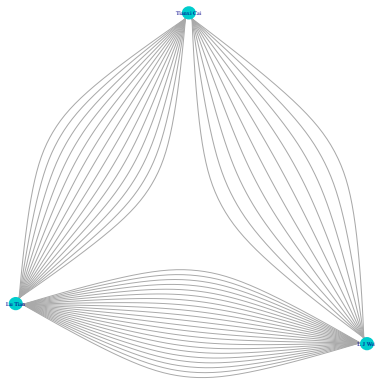


(c) Bayesian statistics community

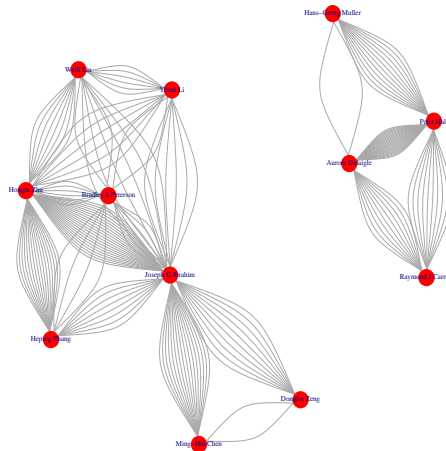
Figure 12: The clustering results for the statisticians' coauthor network by the motif-based spectral clustering. (a) is the general clustering results, and (b) and (c) are specific communities.



(a) Detected communities

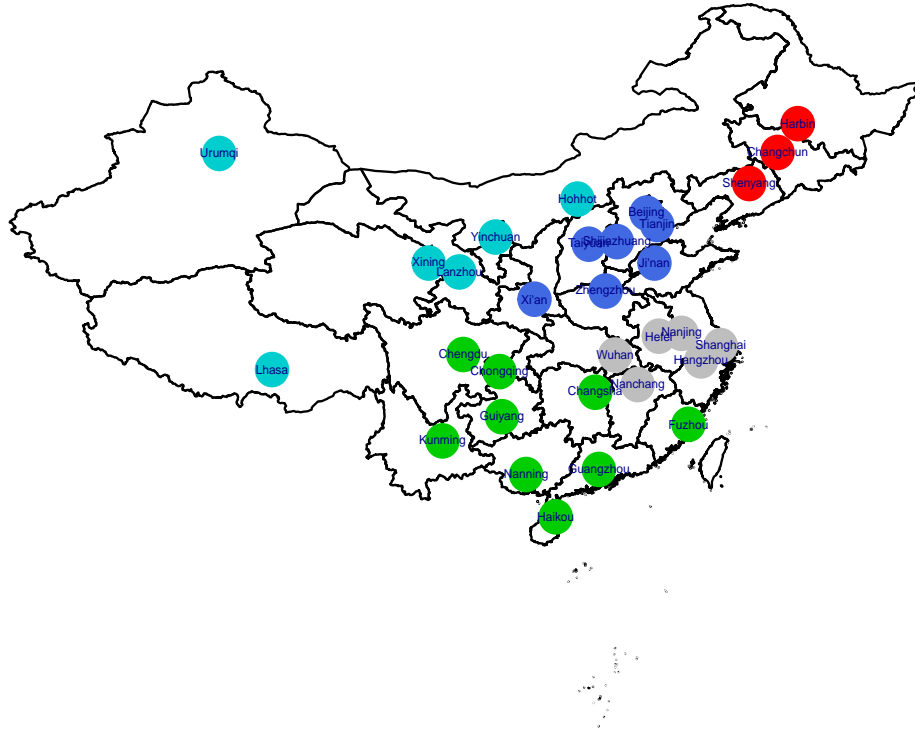


(b) Biostatistics and medical statistics (at Harvard) community



(c) Biostatistics/medical statistics and non-parametric statistics *mixed* community

Figure 13: The clustering results for the statisticians' coauthor network by edge-based spectral clustering. (a) is the general clustering results, and (b) and (c) are specific communities.



(a) Detected communities

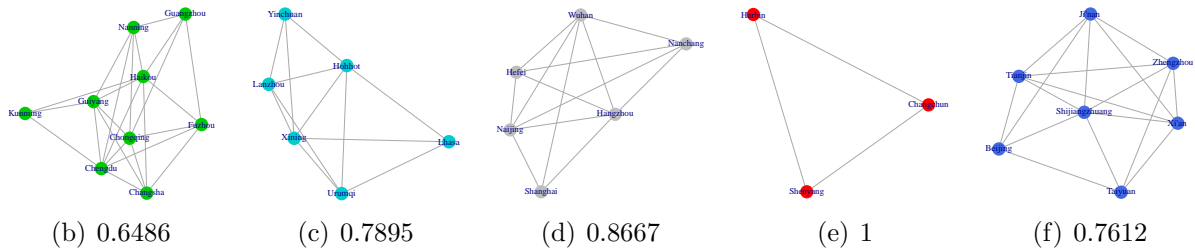
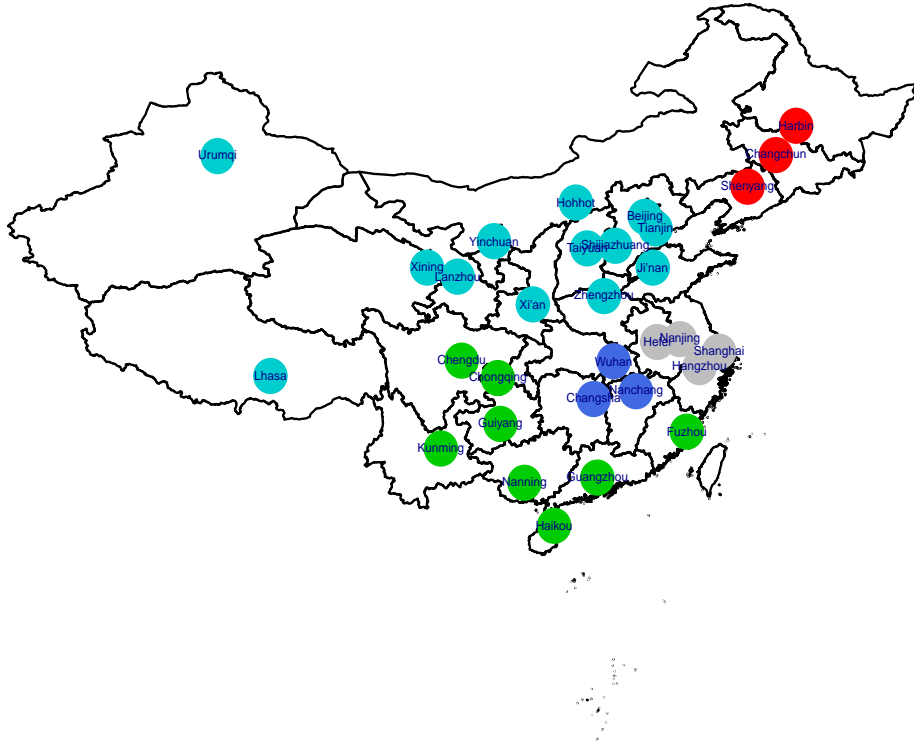


Figure 14: The clustering results for the $PM_{2.5}$ data by the motif-based spectral clustering. (a) is the general clustering results, and (b)-(f) are specific communities where their clustering coefficients are also shown.



(a) Detected communities

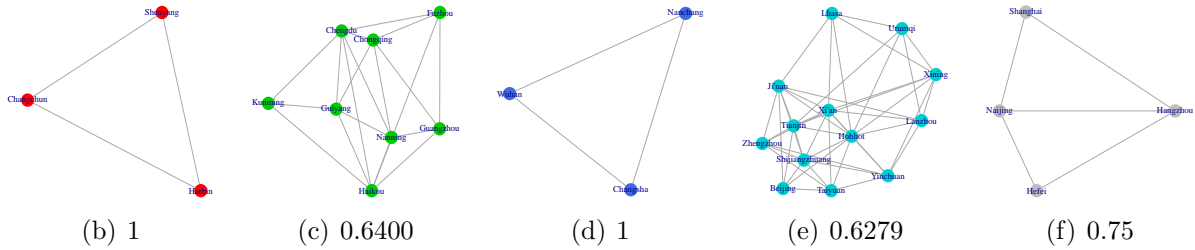


Figure 15: The clustering results for the $PM_{2.5}$ data by the edge-based spectral clustering. (a) is the general clustering results, and (b)-(f) are specific communities where their clustering coefficients are also shown.

References

- Emmanuel Abbe. Community detection and stochastic block models: recent developments. *The Journal of Machine Learning Research*, 18(1):6446–6531, 2018.
- Christopher Aicher, Abigail Z Jacobs, and Aaron Clauset. Learning latent block structure in weighted networks. *Journal of Complex Networks*, 3(2):221–248, 2015.
- Austin R Benson, David F Gleich, and Jure Leskovec. Higher-order organization of complex networks. *Science*, 353(6295):163–166, 2016.
- Rajendra Bhatia. Graduate texts in mathematics: Matrix analysis, 1997.
- Louis Cammarata and Zheng Tracy Ke. Power enhancement and phase transitions for global testing of the mixed membership stochastic block model. *arXiv preprint arXiv:2204.11109*, 2022.
- Andressa Cerqueira and Elizaveta Levina. A pseudo-likelihood approach to community detection in weighted networks. *arXiv preprint arXiv:2303.05909*, 2023.
- Yinghan Chen and Yuguo Chen. An efficient sampling algorithm for network motif detection. *Journal of Computational and Graphical Statistics*, 27(3):503–515, 2018.
- Peter Chin, Anup Rao, and Van Vu. Stochastic block model and community detection in sparse graphs: A spectral algorithm with optimal rate of recovery. In *Conference on Learning Theory*, pages 391–423, 2015.
- Aaron Clauset, Mark EJ Newman, and Cristopher Moore. Finding community structure in very large networks. *Physical review E*, 70(6):066111, 2004.
- Mihai Cucuringu, Huan Li, He Sun, and Luca Zanetti. Hermitian matrices for clustering directed graphs: insights and applications. In *International Conference on Artificial Intelligence and Statistics*, pages 983–992. PMLR, 2020.
- Chandler Davis and William Morton Kahan. The rotation of eigenvectors by a perturbation. iii. *SIAM Journal on Numerical Analysis*, 7(1):1–46, 1970.

- Uriel Feige and Eran Ofek. Spectral techniques applied to sparse random graphs. *Random Structures & Algorithms*, 27(2):251–275, 2005.
- Rina Foygel and Mathias Drton. Extended bayesian information criteria for gaussian graphical models. In *Advances in neural information processing systems*, pages 604–612, 2010.
- Jerome Friedman, Trevor Hastie, and Robert Tibshirani. Sparse inverse covariance estimation with the graphical lasso. *Biostatistics*, 9(3):432–441, 2008.
- Chao Gao, Zongming Ma, Anderson Y Zhang, and Harrison H Zhou. Achieving optimal misclassification proportion in stochastic block models. *The Journal of Machine Learning Research*, 18(1):1980–2024, 2017.
- Debarghya Ghoshdastidar and Ambedkar Dukkipati. Consistency of spectral partitioning of uniform hypergraphs under planted partition model. In *Advances in Neural Information Processing Systems*, pages 397–405, 2014.
- Debarghya Ghoshdastidar and Ambedkar Dukkipati. Uniform hypergraph partitioning: Provable tensor methods and sampling techniques. *The Journal of Machine Learning Research*, 18(1):1638–1678, 2017.
- Debarghya Ghoshdastidar, Ambedkar Dukkipati, et al. Consistency of spectral hypergraph partitioning under planted partition model. *The Annals of Statistics*, 45(1):289–315, 2017.
- Anna Goldenberg, Alice X Zheng, Stephen E Fienberg, Edoardo M Airolidi, et al. A survey of statistical network models. *Foundations and Trends® in Machine Learning*, 2(2): 129–233, 2010.
- Xiao Guo, Yixuan Qiu, Hai Zhang, and Xiangyu Chang. Randomized spectral co-clustering for large-scale directed networks. *arXiv preprint arXiv:2004.12164*, 2020.
- Paul W Holland and Samuel Leinhardt. A method for detecting structure in sociometric data. In *Social Networks*, pages 411–432. Elsevier, 1977.

- Paul W Holland, Kathryn Blackmond Laskey, and Samuel Leinhardt. Stochastic block-models: First steps. *Social networks*, 5(2):109–137, 1983.
- Pengsheng Ji and Jiashun Jin. Coauthorship and citation networks for statisticians. *The Annals of Applied Statistics*, 10(4):1779–1812, 2016.
- Jiashun Jin, Zheng Ke, and Shengming Luo. Network global testing by counting graphlets. In *International conference on machine learning*, pages 2333–2341. PMLR, 2018.
- Jiashun Jin, Zheng Tracy Ke, and Shengming Luo. Optimal adaptivity of signed-polygon statistics for network testing. *The Annals of Statistics*, 49(6):3408–3433, 2021.
- Vishesh Karwa and Aleksandra Slavković. Inference using noisy degrees: Differentially private beta-model and synthetic graphs. *The Annals of Statistics*, 44(1):87–112, 2016.
- Vishesh Karwa, Pavel N Krivitsky, and Aleksandra B Slavković. Sharing social network data: differentially private estimation of exponential family random-graph models. *Journal of the Royal Statistical Society: Series C (Applied Statistics)*, 66(3):481–500, 2017.
- Eric D Kolaczyk. In *Statistical Analysis of Network Data: Methods and Models*. Springer, 2009.
- Steinar Laenen and He Sun. Higher-order spectral clustering of directed graphs. *Advances in Neural Information Processing Systems*, 33:941–951, 2020.
- Jing Lei and Alessandro Rinaldo. Consistency of spectral clustering in stochastic block models. *The Annals of Statistics*, 43(1):215–237, 2015.
- Shmoolik Mangan, Alon Zaslaver, and Uri Alon. The coherent feedforward loop serves as a sign-sensitive delay element in transcription networks. *Journal of molecular biology*, 334(2):197–204, 2003.
- Christopher Manning, Prabhakar Raghavan, and Hinrich Schütze. Introduction to information retrieval. *Natural Language Engineering*, 16(1):100–103, 2010.

- Ron Milo, Shai Shen-Orr, Shalev Itzkovitz, Nadav Kashtan, Dmitri Chklovskii, and Uri Alon. Network motifs: simple building blocks of complex networks. *Science*, 298(5594): 824–827, 2002.
- Mark Newman. *Networks*. Oxford university press, 2018.
- Mark EJ Newman. Modularity and community structure in networks. *Proceedings of the national academy of sciences*, 103(23):8577–8582, 2006.
- Subhadeep Paul and Yuguo Chen. Spectral and matrix factorization methods for consistent community detection in multi-layer networks. *Annals of Statistics*, 48(1):230–250, 2020.
- Subhadeep Paul, Olgica Milenkovic, and Yuguo Chen. Higher-order spectral clustering under superimposed stochastic block model. *arXiv preprint arXiv:1812.06515*, 2018.
- Carey E Priebe, Youngser Park, Joshua T Vogelstein, John M Conroy, Vince Lyzinski, Minh Tang, Avanti Athreya, Joshua Cape, and Eric Bridgeford. On a two-truths phenomenon in spectral graph clustering. *Proceedings of the National Academy of Sciences*, 116(13): 5995–6000, 2019.
- Tai Qin and Karl Rohe. Regularized spectral clustering under the degree-corrected stochastic blockmodel. In *Advances in Neural Information Processing Systems*, pages 3120–3128, 2013.
- K Rohe and T Qin. The blessing of transitivity in sparse and stochastic networks. *arXiv*, pages 1–29, 2013.
- Karl Rohe, Sourav Chatterjee, and Bin Yu. Spectral clustering and the high-dimensional stochastic block model. *The Annals of Statistics*, 39(4):1878–1915, 2011.
- Martin Rosvall, Alcides V Esquivel, Andrea Lancichinetti, Jevin D West, and Renaud Lambiotte. Memory in network flows and its effects on spreading dynamics and community detection. *Nature communications*, 5:4630, 2014.

- Belkacem Serrou, Alex Arenas, and Sergio Gómez. Detecting communities of triangles in complex networks using spectral optimization. *Computer Communications*, 34(5):629–634, 2011.
- C Seshadhri, Ali Pinar, and Tamara G Kolda. Wedge sampling for computing clustering coefficients and triangle counts on large graphs. *Statistical Analysis and Data Mining: The ASA Data Science Journal*, 7(4):294–307, 2014.
- Charalampos E Tsourakakis, Jakub Pachocki, and Michael Mitzenmacher. Scalable motif-aware graph clustering. In *Proceedings of the 26th International Conference on World Wide Web*, pages 1451–1460. International World Wide Web Conferences Steering Committee, 2017.
- William G Underwood, Andrew Elliott, and Mihai Cucuringu. Motif-based spectral clustering of weighted directed networks. *Applied Network Science*, 5(1):1–41, 2020.
- Ulrike Von Luxburg. A tutorial on spectral clustering. *Statistics and computing*, 17(4):395–416, 2007.
- Bo Wang, Armin Pourshafeie, Marinka Zitnik, Junjie Zhu, Carlos D Bustamante, Serafim Batzoglou, and Jure Leskovec. Network enhancement as a general method to denoise weighted biological networks. *Nature communications*, 9(1):1–8, 2018.
- Lutz Warnke. On the method of typical bounded differences. *Combinatorics, Probability and Computing*, 25(2):269–299, 2016.
- Lutz Warnke. Upper tails for arithmetic progressions in random subsets. *Israel Journal of Mathematics*, 221(1):317–365, 2017.
- Min Xu, Varun Jog, and Po-Ling Loh. Optimal rates for community estimation in the weighted stochastic block model. *The Annals of Statistics*, 48(1):183–204, 2020.
- Jaewon Yang and Jure Leskovec. Overlapping communities explain core–periphery organization of networks. *Proceedings of the IEEE*, 102(12):1892–1902, 2014.

Hao Yin, Austin R Benson, Jure Leskovec, and David F Gleich. Local higher-order graph clustering. In *Proceedings of the 23rd ACM SIGKDD international conference on knowledge discovery and data mining*, pages 555–564, 2017.

Ming Yuan and Yi Lin. Model selection and estimation in the gaussian graphical model. *Biometrika*, 94(1):19–35, 2007.

Hai Zhang, Xiao Guo, and Xiangyu Chang. Randomized spectral clustering in large-scale stochastic block models. *Journal of Computational and Graphical Statistics*, 31(3):887–906, 2022.